Cell Reports
Medicine

Article

Entrectinib inhibits NLRP3 inflammasome and inflammatory diseases by directly targeting NEK7

Graphical abstract

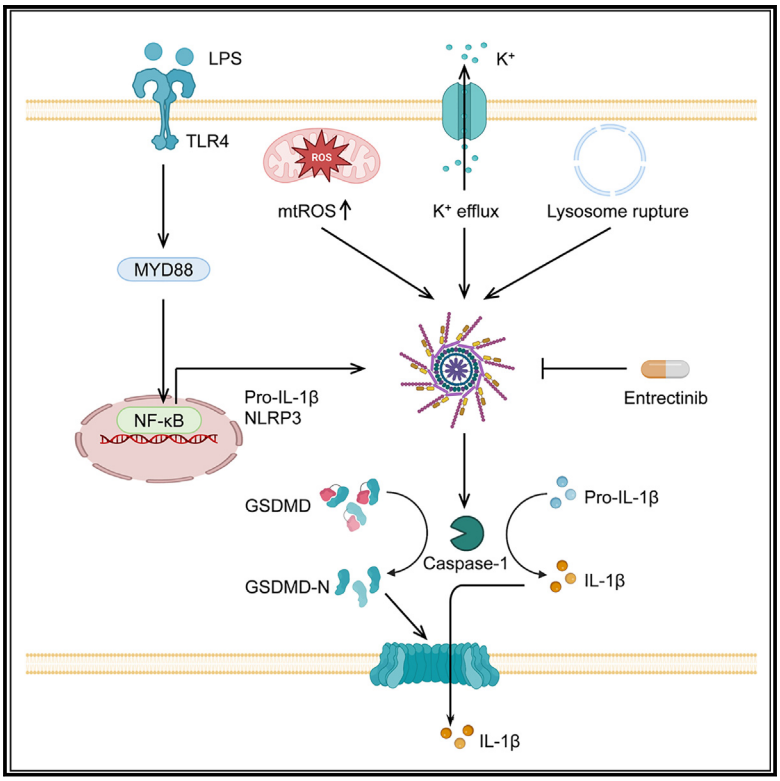

Authors

Xiangyu Jin, Didi Liu, Xinru Zhou, Xianyu Luo, Qian Huang, Yi Huang

Correspondence

hy527@ustc.edu.cn

In brief

Jin et al. identify that entrectinib specifically blocks activation of the NLRP3 inflammasome by directly binding to arginine 121 of NEK7. Entrectinib has a significant ameliorative effect on mouse models of NLRP3 inflammasome-related diseases, including systemic inflammation, peritonitis, and type 2 diabetes.

Highlights

- Entrectinib specifically inhibits NLRP3 inflammasome activation
- Entrectinib is a targeted inhibitor of NEK7 and binds directly to its R121 residue
- Entrectinib blocks the NLRP3-NEK7 interaction and inflammasome assembly
- Entrectinib demonstrates a beneficial impact on NLRP3 inflammasome-related diseases

Jin et al., 2023, Cell Reports Medicine *4*, 101310
December 19, 2023
https://doi.org/10.1016/j.xcrm.2023.101310

CellPress

Cell Reports Medicine

CellPress
OPEN ACCESS

Article

Entrectinib inhibits NLRP3 inflammasome and inflammatory diseases by directly targeting NEK7

Xiangyu Jin,[1,2,3] Didi Liu,[2,3] Xinru Zhou,[2] Xianyu Luo,[2] Qian Huang,[2] and Yi Huang[1,2,4,*]
[1]Insitute of Health and Medicine, Hefei Comprehensive National Science Center, Hefei 230601, China
[2]Wuxi School of Medicine, Jiangnan University, Jiangsu, China
[3]These authors contributed equally
[4]Lead contact
*Correspondence: hy527@ustc.edu.cn
https://doi.org/10.1016/j.xcrm.2023.101310

SUMMARY

Excessive inflammation caused by abnormal activation of the NLRP3 inflammasome contributes to the pathogenesis of multiple human diseases, but clinical drugs targeting the NLRP3 inflammasome are still not available. In this study, we identify entrectinib (ENB), a US Food and Drug Administration (FDA)-approved anticancer agent, as a target inhibitor of the NLRP3 inflammasome to treat related diseases. ENB specifically blocks NLRP3 without affecting activation of other inflammasomes. Furthermore, we demonstrate that ENB directly binds to arginine 121 (R121) of NEK7 and blocks the interaction between NEK7 and NLRP3, thereby inhibiting inflammasome assembly and activation. *In vivo* studies show that ENB has a significant ameliorative effect on mouse models of NLRP3 inflammasome-related diseases, including lipopolysaccharide (LPS)-induced systemic inflammation, monosodium urate (MSU)-induced peritonitis, and high-fat diet (HFD)-induced type 2 diabetes (T2D). These data show that ENB is a targeted inhibitor of NEK7 with strong anti-NLRP3 inflammasome activity, making it a potential candidate drug for the treatment of inflammasome-related diseases.

INTRODUCTION

The nod-like receptors (NLRs) are a class of pattern recognition receptors (PRRs) in the cytoplasm, and several members of the family, including NLRP1, NLRP3, NLRP6, Pyrin, and CARD8, have been reported to form a protein complex called the inflammasome and mediate the inflammatory response.[1,2] NLRP3 is one of the most important NLRs and can recognize not only pathogen-associated molecular patterns (PAMPs; for example, viral RNAs, microbial toxins, and nigericin) but also damage-associated molecular patterns (DAMPs), such as monosodium urate (MSU) crystals, amyloids, ATP, and cholesterol crystals.[3–6] Upon stimulation by those PAMPs and DAMPs, NLRP3 first binds to NEK7 and subsequently recruits the cysteine protease pro-caspase-1 via the adapter protein apoptosis-associated speck-like protein containing a caspase recruitment domain (ASC) to form the inflammasome.[7–9] The assembled NLRP3 inflammasome induces pro-caspase-1 self-cleavage and activation. Then, the activated caspase-1 not only cleaves pro-interleukin-1β (IL-1β) and pro-IL-18 to produce mature IL-1β- and IL-18-mediated inflammatory responses but also cleaves gasdermin D (GSDMD) to induce pyroptosis, which is crucial for host defense against pathogens and maintaining homeostasis.[10–13] However, excessive activation of the NLRP3 inflammasome can also lead to multiple inflammatory diseases, including peritonitis, atherosclerosis, type 2 diabetes (T2D), experimental autoimmune encephalomyelitis (EAE), and neurodegenerative disease.[14–17] Therefore, the NLRP3 inflammasome is a promising drug target for the treatment of those inflammatory diseases.

In recent years, some small-molecule compounds have been found to improve inflammatory diseases by targeting the NLRP3 inflammasome.[18] MCC950, CY-09, tranilast, tivantinib, and oridonin have been reported to interact directly with NLRP3 to inhibit the assembly and activation of inflammasomes, thereby alleviating immune responses and inflammatory diseases, such as sepsis, peritonitis, T2D, and EAE.[19–24] In addition to targeting NLRP3, sennoside A, CZL80, and a selective and irreversible inhibitor of caspase-1 (Ac-YVAD-cmk) have been found to inhibit inflammasome activation by blocking the activity of caspase-1 and have shown favorable anti-inflammatory effects in animal models.[25–27] Moreover, targeted inhibitors of GSDMD, such as necrosulfonamide (NSA), disulfiram (DSF), dimethyl fumarate (DMF), and fumarate have also been found to alleviate a variety of inflammatory diseases by inhibiting inflammasome activation.[28–30] As an important component of the NLRP3 inflammasome, NEK7 is also an attractive target for inflammasome activation and treatment of related diseases. HT-6184 and MRT-3483 are two NEK7 inhibitors identified in 2022 by Halia Therapeutics and Monte Rosa Therapeutics, respectively, for the treatment of inflammatory diseases;

MRT-3483 is currently in the preclinical stage, and HT-6184 is in phase I clinical trials to evaluate safety and tolerability (ClinicalTrials.gov: NCT05447546). Therefore, it will be a long time before these compounds are available for clinical use, and there is an urgent need to develop other NEK7-targeting drugs with high safety and specificity that are closer to clinical application.

Entrectinib (ENB) is a potent tyrosine multikinase small-molecule inhibitor that targets the oncogenes neurotrophic tropomyosin receptor kinase (NTRK), c-ROS oncogene 1 (ROS1), and anaplastic lymphoma kinase (ALK).[31] In 2019, ENB was approved by the US Food and Drug Administration (FDA) for the treatment of adults and pediatric patients 12 years of age and older with solid tumors that have an NTRK gene fusion. Furthermore, it has now been approved for the treatment of adults with metastatic non-small cell lung cancer (NSCLC) whose tumors are ROS1 positive.[32] Clinical studies have shown that ENB has a significant anti-cancer effect, which results in durable disease control and prolonged progression-free survival.[31,33] ENB is a clinical drug that can cross the blood-brain barrier with a half-life of elimination of 20 h.[31] More importantly, ENB has a high safety profile and is well tolerated by almost all patients without cumulative toxicity, even at doses up to 600 mg orally once a day continuously for 3 months.[34]

In this study, we identified that ENB significantly inhibits NLRP3 inflammasome activation by screening the clinical or FDA-approved kinase inhibitors in our lab. Mechanistic studies revealed that ENB directly targets NEK7 at R121, blocking NEK7-NLRP3 interaction and subsequent inflammasome assembly and activation. Furthermore, ENB showed significant therapeutic effects in multiple mouse models of NLRP3 inflammasome-driven diseases, including lipopolysaccharide (LPS)-induced systemic inflammation, peritonitis, and T2D, suggesting that ENB may be a promising candidate for the treatment of these inflammatory diseases.

RESULTS

Identification of ENB as a potent inhibitor of the NLRP3 inflammasome

To identify drugs that inhibit NLRP3 inflammasome activation, we screened 195 clinical or FDA-approved kinase inhibitors in our lab and found that ENB was highly effective in inhibiting inflammasome activation in mouse primary bone marrow-derived macrophages (BMDMs) (Figures S1A and S1B; Table S1). ENB is a clinical anti-cancer agent approved by the FDA for the treatment of multiple solid tumors and is not cytotoxic to BMDMs even at higher concentrations (Figure S1C). The half-maximal inhibitory concentration (IC_{50}) of ENB for MSU-induced IL-1β production was approximately 0.88 μM, which was similar to the IC_{50} of nigericin-induced (IC_{50} = 0.65 μM) and ATP-induced (IC_{50} = 0.73 μM) IL-1β production (Figures 1A–1C). In addition to inducing IL-1β maturation, NLRP3 inflammasome activation also promote pyroptosis.[10–12] We found that ENB dose-dependently inhibited MSU- and nigericin-induced lactate dehydrogenase (LDH) release (Figures S1D and S1E). Moreover, nigericin-induced cell death and GSDMD cleavage were also potently blocked by ENB (Figures S1F–S1H). These results indicate that ENB inhibits NLRP3 inflammasome activation and pyroptosis.

In addition to MSU, nigericin, and ATP, we also examined the inhibitory effect of ENB on inflammasome activation induced by other NLRP3 stimuli, including imiquimod,[35] alum,[36,37] and SiO_2.[38] The results showed that ENB significantly inhibited IL-1β secretion and caspase-1 cleavage in response to those stimuli (Figures 1D and 1E). Previous studies have shown that intracellular LPS induces caspase-11-dependent non-canonical inflammasome activation, where IL-1β but not LDH release requires NLRP3.[13,39,40] We pretreated pam3CSK4-primed BMDMs with different concentrations of ENB, followed by transfection with LPS, and found that ENB inhibited IL-1β secretion and caspase-1 cleavage in a dose-dependent manner without affecting LDH release (Figures 1F, 1G, and S2A). Consistent with these results, we found that ENB could also inhibit IL-1β secretion and caspase-1 cleavage in human THP-1 cells and peripheral blood mononuclear cells (PBMCs) in a dose-dependent manner (Figures 1H, 1I, S2B, and S2C). Taken together, these results suggest that ENB is a common inhibitor of the NLRP3 inflammasome.

ENB specifically inhibits NLRP3 without affecting activation of other inflammasomes

To investigate the specific effect of ENB on NLRP3 inflammasome activation, we pretreat LPS-primed BMDMs with ENB and then induced AIM2 inflammasome activation by transfection with poly(dA:dT).[41,42] The results showed that ENB had no effect on poly(dA:dT)-induced caspase-1 cleavage or IL-1β secretion (Figures 2A and 2B). Similarly, ENB could also not inhibit NLRC4 inflammasome activation induced by *Salmonella enterica* Typhimurium (*Salmonella*) infection[43] (Figures 2C and 2D). In addition to NLRP3, AIM2, and NLRC4, emerging evidence suggests that Pyrin, NLRP1, NLRP6, and CARD8 are also capable of forming inflammasomes.[1] We next explored whether ENB inhibited these types of inflammasome activation and found that ENB did not affect either *Clostridium difficile* toxin B (TcdB)-induced Pyrin[44] and *Listeria monocytogenes* (*Listeria*)-induced NLRP6[45] inflammasome activation or Val-boroPro (VbP)-induced NLRP1 and CARD8 inflammasome activation (Figures 2E and 2F). In conclusion, these results suggest that ENB specifically inhibits NLRP3 without affecting activation of other inflammasomes. We then examined whether ENB had an effect on the priming phase of NLRP3 inflammasome activation. BMDMs were treated with different concentrations of ENB before LPS stimulation, and we found that ENB did not affect LPS-induced pro-IL-1β or NLRP3 expression (Figure 2G). Furthermore, ENB also had no effect on LPS-induced tumor necrosis factor alpha (TNF-α) or IL-6 secretion (Figures 2H and 2I), suggesting that ENB did not affect the priming step of NLRP3 activation. Together, these data demonstrate that ENB is a specific inhibitor of the NLRP3 inflammasome.

Since a few compounds, including MCC950,[23] CY-09,[24] tranilast,[21] tivantinib,[19] and β-hydroxybutyrate (BHB),[46] have been reported recently to inhibit NLRP3 inflammasome activation, we therefore compared the inhibitory effect and specificity of ENB with these compounds on NLRP3 inflammasome activation. The IC_{50} of these compounds on nigericin-induced IL-1β production were tested, and we found that ENB had an effect comparable with tivantinib and superior to CY-09, tranilast, and BHB in

CellPress
OPEN ACCESS

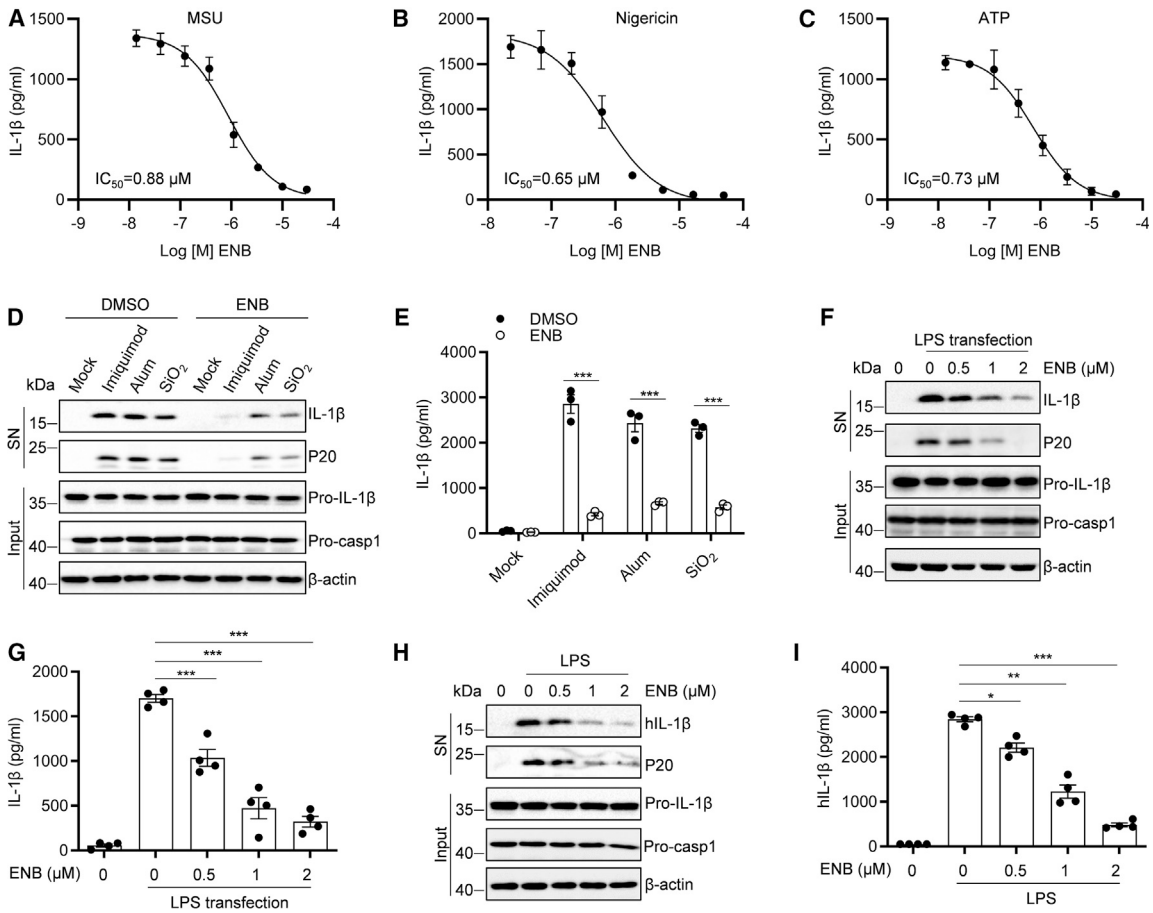

Figure 1. Identification of ENB as a potent inhibitor of the NLRP3 inflammasome

(A–C) ELISA analysis of IL-1β in culture supernatants (SNs) from LPS-primed BMDMs treated with various doses of ENB and then stimulated with 150 μg/mL MSU for 4 h (A), 5 μM nigericin (B), or 2.5 mM ATP (C) for 30 min.

(D) Immunoblot analysis of IL-1β and cleaved caspase-1 (P20) in SN, pro-IL-1β and pro-caspase-1 (Pro-casp1) in cell lysates (input) from LPS-primed BMDMs treated with 2 μM ENB and then stimulated with 15 μg/mL imiquimod for 3 h or 300 μg/mL alum or SiO_2 for 6 h.

(E) ELISA of IL-1β in SNs from LPS-primed BMDMs treated with 2 μM ENB and then stimulated with 15 μg/mL imiquimod for 3 h or 300 μg/mL alum or SiO_2 for 6 h.

(F) Immunoblot analysis of IL-1β and P20 in SNs and pro-IL-1β and pro-casp1 in input from Pam3CSK4-primed BMDMs treated with various doses of ENB and then transfected with 0.5 μg/mL LPS for 16 h.

(G) ELISA of IL-1β in SN from Pam3CSK4-primed BMDMs treated with various doses of ENB and then transfected with 0.5 μg/mL LPS for 16 h.

(H) Immunoblot analysis of IL-1β and P20 in SNs and pro-IL-1β and pro-casp1 in input from PBMCs treated with various doses of ENB and then stimulated with 1 μg/mL LPS for 24 h.

(I) ELISA of IL-1β in SNs from PBMCs treated with various doses of ENB and then stimulated with 1 μg/mL LPS for 24 h.

Data represent the mean ± SEM of three (A–C and E) or four (G and I) technical replicates from one of five independent experiments. Statistical analysis was performed using one-way ANOVA (G and I) or two-way ANOVA (E). *p < 0.05, **p < 0.01, ***p < 0.001.

inhibiting NLRP3 inflammasome activation. However, MCC950 showed the best inhibitory effect among all compounds (Figures S3A–S3E). Previous studies have shown that tranilast[21] and BHB[46] can inhibit nuclear factor κB (NF-κB) signaling, which was validated by our results. Moreover, we found that tivantinib inhibited IL-6 release and pro-IL-1β expression when it was used prior to LPS priming (Figures S3F and S3G), indicating that tivantinib has a broad anti-inflammatory effect rather than specifically inhibiting NLRP3 inflammasome activation. Although MCC950 appears to be a specific inhibitor of NLRP3, it has been tested previously tested in a phase II clinical trial for rheumatoid arthritis (RA) and found to elevate liver enzyme levels in serum, suggesting that it may have liver toxicity.[47] In contrast, ENB is an FDA-approved anti-cancer agent with a high safety profile,[32] and our results also confirmed that ENB had no side effects on the heart, liver, spleen, lungs, and kidneys of mice even with continuous administration for 3 months (Figure S3H). Together, these results suggest that ENB is a safe, potent, and specific inhibitor of the NLRP3 inflammasome.

ENB inhibits NLRP3 inflammasome activation by directly targeting NEK7

We then explored the mechanism by which ENB inhibits activation of the NLRP3 inflammasome. As an excellent anti-cancer

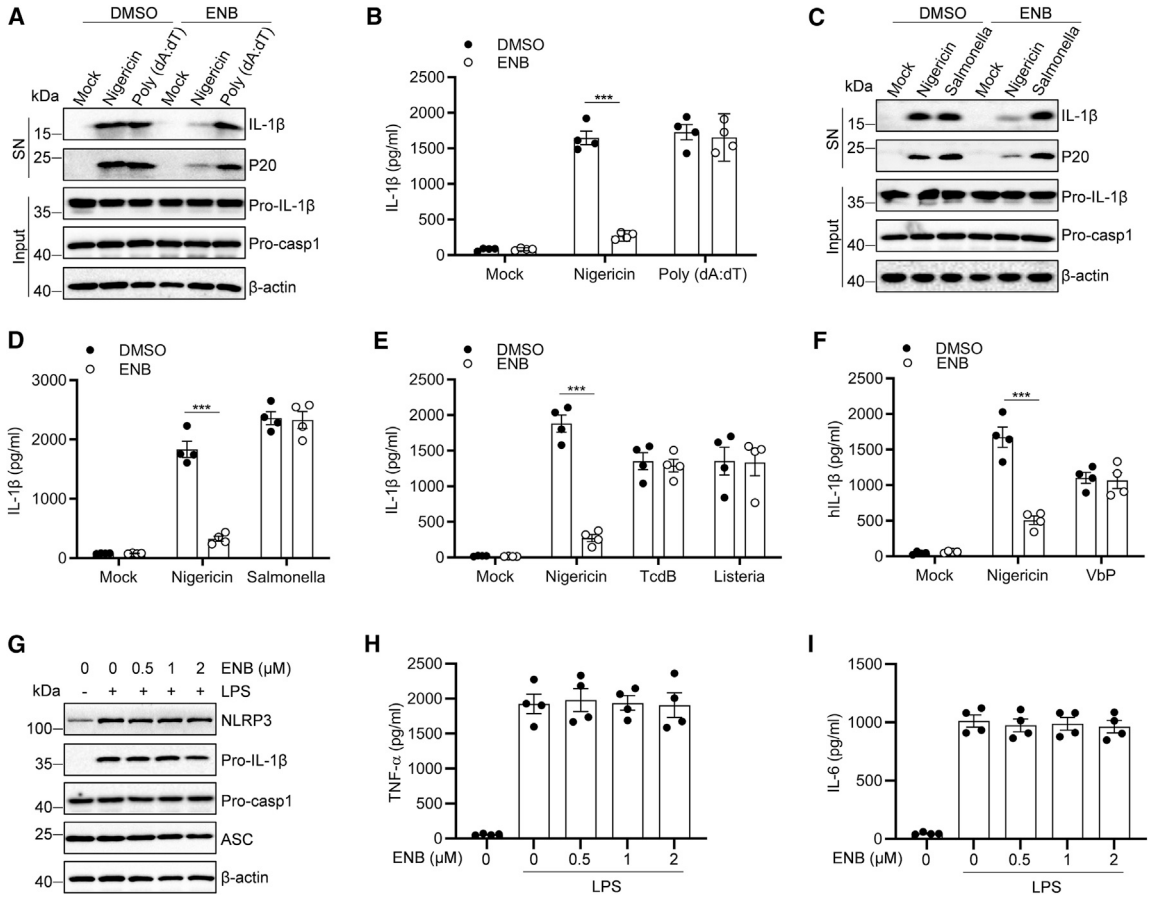

Figure 2. ENB specifically inhibits NLRP3 without affecting activation of other inflammasomes

(A) Immunoblot analysis of IL-1β and P20 in SNs and pro-IL-1β and pro-casp1 in input from LPS-primed BMDMs treated with 2 μM ENB and then stimulated with 5 μM nigericin for 30 min or transfected with 0.5 μg/mL poly(dA:dT) for 4 h.

(B) ELISA of IL-1β in SNs from LPS-primed BMDMs treated with 2 μM ENB and then stimulated with 5 μM nigericin for 30 min or transfected with 0.5 μg/mL poly(dA:dT) for 4 h.

(C) Immunoblot analysis of IL-1β and P20 in SNs and pro-IL-1β and Pro-casp1 in input from LPS-primed BMDMs treated with 2 μM ENB and then stimulated with 5 μM nigericin for 30 min or infected with *Salmonella* (multiplicity of infection [MOI] = 5) for 4 h.

(D) ELISA of IL-1β in SNs from LPS-primed BMDMs treated with 2 μM ENB and then stimulated with 5 μM nigericin for 30 min or infected with *Salmonella* (MOI = 5) for 4 h.

(E) ELISA of IL-1β in SNs from LPS-primed BMDMs treated with 2 μM ENB and then stimulated with 5 μM nigericin for 30 min or 0.5 μg/mL *C. difficile* toxin B (TcdB) for 1 h or infected with *L. monocytogenes* (*Listeria*; MOI = 10) for 4 h.

(F) ELISA of IL-1β in SNs from phorbol 12-myristate 13-acetate (PMA)-differentiated and LPS-primed THP-1 cells treated with 2 μM ENB and then stimulated with 5 μM nigericin for 1 h or 10 μM Val-boroPro (VbP) for 24 h.

(G) Immunoblot analysis of NLRP3 and pro-IL-1β in input from BMDMs treated with various doses of ENB and then stimulated with 50 ng/mL LPS for 3 h.

(H and I) ELISA of TNF-α (H) and IL-6 (I) in SNs from BMDMs treated with various doses of ENB and then stimulated with 50 ng/mL LPS for 3 h.

Data represent the mean ± SEM of four technical replicates from one of five independent experiments. Statistical analysis was performed using two-way ANOVA (B and D–F). ***$p < 0.001$.

drug, ENB has been reported to inhibit tumor growth by blocking multiple kinases, including NTRK, ROS1 and ALK.[31,34] To investigate whether the inhibitory effect of ENB on NLRP3 inflammasome activation is also dependent on these targets, we first pretreated LPS-primed BMDMs with inhibitors of NTRK and ALK, including repotrectinib, belizatinib, and larotrectinib, and then stimulated the cells with nigericin. The results showed that these inhibitors had no effect on NLRP3 inflammasome activation (Figures S4A and S4B). Moreover, we knocked down ROS1 with small interfering RNA (siRNA) and found that ROS1 knockdown neither affected NLRP3 inflammasome activation nor reversed the inhibitory effect of ENB (Figures S4C–S4E). These results suggest that the inhibitory effect of ENB on NLRP3 inflammasome activation is independent of the previously reported targets.

Although the detailed mechanism of NLRP3 inflammasome activation is not yet well understood, several events, including potassium and chloride efflux, mitochondrial damage, and reactive oxygen species (ROS) production, are widely accepted as key upstream signals of its activation.[48] We first studied whether

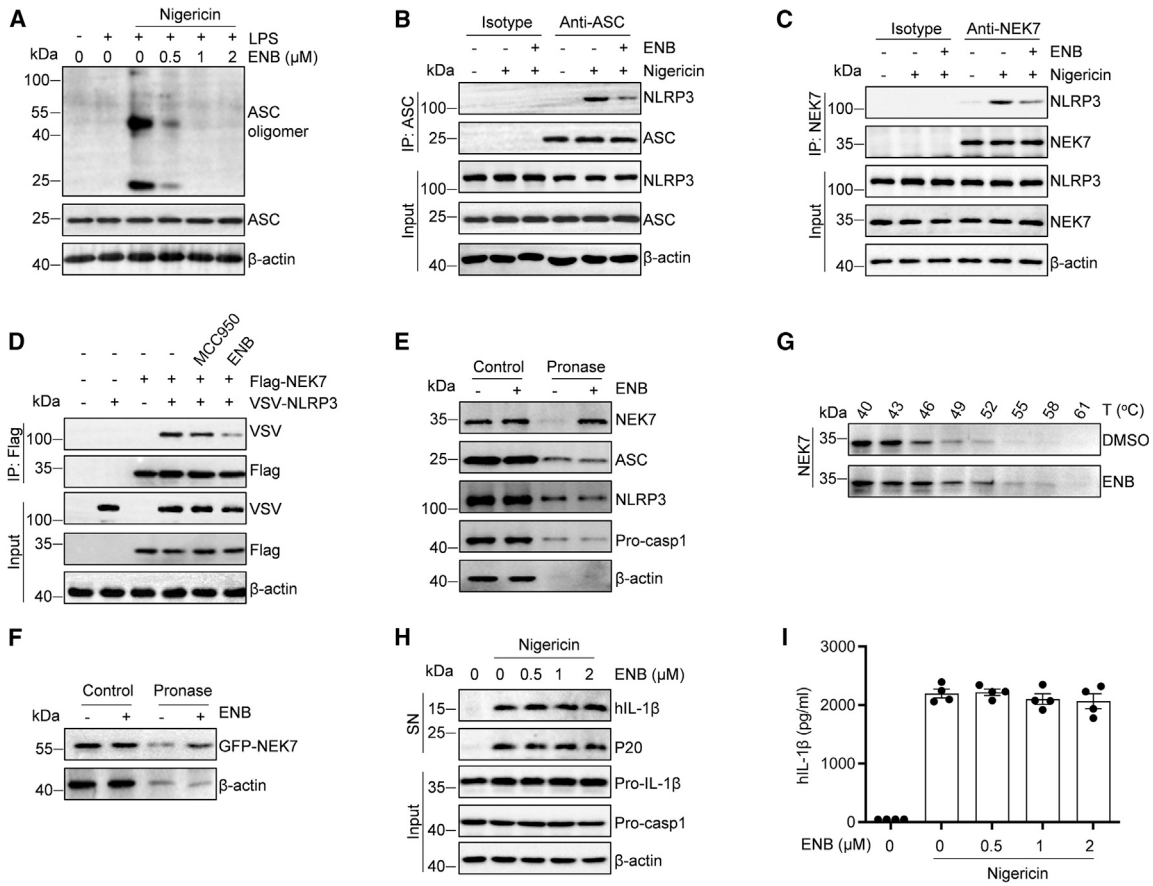

Figure 3. ENB suppresses NLRP3 inflammasome assembly by directly targeting NEK7

(A) Immunoblot analysis of ASC oligomerization in cross-linked cytosolic pellets of LPS-primed BMDMs treated with various doses of ENB and then stimulated with 5 μM nigericin for 30 min.

(B and C) Immunoprecipitation (IP) and immunoblot analysis of the interaction between endogenous ASC (B) or NEK7 (C) and NLRP3 in LPS-primed BMDMs treated with 2 μM ENB and then stimulated with 5 μM nigericin for 30 min.

(D) IP and immunoblot analysis of HEK293T cells transfected with VSV-NLRP3, FLAG-NEK7, or empty vector plasmids as indicated and treated with 2 μM ENB or 1 μM MCC950.

(E) Drug affinity responsive target stability (DARTS) and immunoblot analysis of NEK7, NLRP3, ASC, and pro-casp1 in LPS-primed BMDMs treated with 200 μM ENB and then performed with pronase (25 ng/μg of protein).

(F) DARTS and immunoblot analysis of NEK7 in HEK293T cells transfected with GFP-NEK7 and then treated with 200 μM ENB and pronase (25 ng/μg of protein).

(G) Cellular thermal shift assays (CETSAs) and immunoblot analysis of NEK7 stability in LPS-primed BMDMs treated with 200 μM ENB at different temperatures.

(H) Immunoblot analysis of IL-1β and P20 in SNs, pro-IL-1β, and pro-casp1 in input from pam3CSK4-primed human BLaER1 monocytes treated with various doses of ENB and then stimulated with 5 μM nigericin for 2 h.

(I) ELISA of IL-1β in SNs from pam3CSK4-primed human BLaER1 monocytes treated with various doses of ENB and then stimulated with 5 μM nigericin for 2 h. Data represent the mean ± SEM of four technical replicates from one of five independent experiments (I).

ENB affected potassium efflux, and the results showed that treatment of BMDMs with nigericin significantly reduced intracellular potassium concentration, but ENB could not reverse potassium efflux (Figure S5A), suggesting that ENB has no effect on potassium efflux during NLRP3 inflammasome activation. Similarly, ENB was also not able to relieve the chloride efflux induced by nigericin (Figure S5B). Next, to explore the effect of ENB on mitochondrial damage and mitochondrial ROS production, we stained for mitochondrial oxidation with MitoSOX and mitochondrial damage with MitoTracker, and the results showed that ENB could not inhibit mitochondrial damage or ROS production during NLRP3 inflammasome activation (Figure S5C). Thus, these results suggest that ENB inhibits NLRP3 inflammasome activation downstream of potassium and chloride efflux, mitochondrial damage, and ROS production.

Because ENB had no effect on the common upstream signals of NLRP3 inflammasome activation, we hypothesized that it may directly inhibit assembly of the NLRP3 inflammasome. ASC oligomerization has been reported to be one of the most downstream steps in inflammasome assembly. Our results showed that ENB inhibited nigericin-induced ASC oligomerization in a dose-dependent manner (Figure 3A). Recruitment of ASC by NLRP3 is a critical step of inflammasome formation. We examined the interaction between NLRP3 and ASC and found that

ENB significantly inhibits the endogenous NLRP3-ASC interaction in BMDMs but has no effect on exogenous NLRP3-ASC interaction in HEK293T cells transfected with vesicular stomatitis virus (VSV)-NLRP3 and FLAG-ASC (Figures 3B and S5D), indicating that ENB inhibits NLRP3 inflammasome assembly by acting upstream of the NLRP3-ASC interaction. Further studies showed that ENB inhibited endogenous and exogenous NLRP3-NEK7 interaction but did not affect exogenous NLRP3-NLRP3 interaction (Figures 3C, 3D, and S5E). These results suggest that ENB may specifically block NLRP3 binding to NEK7.

Next, we sought to identify the target protein of ENB. Because ENB inhibits NLRP3-NEK7 interaction, we hypothesized that it might target NLRP3 or NEK7. By using the drug affinity responsive target stability (DARTS) technique, a method based on the reduction of protease sensitivity of the target protein in response to drug binding,[49] we found that ENB protected NEK7 from protease-mediated proteolysis but does not affect the proteolysis of other components of the NLRP3 inflammasome, including NLRP3, ASC, and pro-caspase-1, in the presence of protease pronase (Figure 3E). Similarly, NEK7 proteolysis was also significantly inhibited by ENB in HEK293T cells overexpressing GFP-NEK7 (Figure 3F). To further confirm this result, we conducted a cellular thermal shift assay (CETSA) in BMDMs, a method that allows studies of target engagement of the drug target in a cellular context.[50] The results showed that ENB significantly enhanced the thermal stability of NEK7 even at higher temperatures compared with the DMSO-treated group (Figure 3G), indicating that ENB binds to NEK7. Recent studies have revealed that NEK7 is dispensable for NLRP3 inflammasome activation in human BLaER1 cells.[51] We examined the effect of ENB on NLRP3 inflammasome activation in BLaER1 cells and found that ENB did not inhibit nigericin-induced caspase-1 cleavage and IL-1β release, confirming that ENB inhibits NLRP3 inflammasome activation by targeting NEK7 (Figures 3H and 3I). Thus, these results indicate that ENB directly targets NEK7 to inhibit NLRP3-NEK7 interaction and NLRP3 inflammasome assembly and activation.

ENB binds to the R121 residue of NEK7

To explore the nature of the interaction between ENB and NEK7, we sought to determine whether the inhibitory effect of ENB on NLRP3 inflammasome activation is reversible. We pretreated LPS-primed BMDMs with ENB for 15 min and then washed the cells three times to remove the unbound drug before nigericin stimulation. The results showed that ENB could not inhibit the production of IL-1β after washout (Figure 4A), indicating that the inhibitory effect of ENB on NLRP3 inflammasome activation is reversible. To further identify which residues on NEK7 bind to ENB, we investigated the molecular interaction of ENB and template structure of human NEK7 (PDB: 6S76) by AutoDock4. The results showed that ENB was readily docked into the NEK7 pocket with −5.79 kcal/mol binding energy (Figure 4B). Moreover, ENB was predicted to bind to NEK7 by hydrogen bonding at isoleucine 40 (I40) and R121 (Figure 4C). Next, DARTS was performed in HEK293T cells overexpressing wild-type (WT) or mutant NEK7 plasmids. We found that R121A, but not I40A mutation, abolished NEK7 binding to ENB (Figure 4D), suggesting that ENB binds to R121 of NEK7.

Interestingly, it has been found previously that the R121 residue of NEK7 is located at the interaction interface between NEK7 and NLRP3.[8] We performed a co-immunoprecipitation assay in HEK293T cells transfected with NLRP3 and NEK7 R121A mutant plasmids and then treated them with ENB. The results showed that the R121A mutation significantly inhibited the interaction between NLRP3 and NEK7, but the inhibition effect was not further enhanced by ENB treatment (Figure 4E). Moreover, we found that ENB inhibits NLRP3 inflammasome activation in NEK7 knockout THP-1 cells recombined with human WT NEK7 but not R121A mutant NEK7 (Figure 4F). These results indicate that the R121 residue of NEK7 is essential for ENB to inhibit NLRP3 inflammasome activation. Because the R121 residue is well conserved in different organisms (Figure S6A), we subsequently confirmed the importance of this site in NEK7-deficient murine immortalized bone marrow-derived macrophages (iBMDMs). The results showed that ENB had no effect on activation of the NLRP3 inflammasome in NEK7 R121A mutant cells (Figures 4G and 4H). Thus, these results indicate that ENB inhibits NLRP3 inflammasome activation by binding to the R121 residue of NEK7.

Next, we investigated the binding and functional specificity of ENB to NEK7. Previous studies have shown that NEK6 and NEK9, two other members of the NEK family, are highly homologous to NEK7.[52] We analyzed the conservation of R121 in NEK6 and NEK9 and found that R121 is absent in these two proteins (Figure S6B). Furthermore, we found that ENB binds only to NEK7, but not to NEK6 or NEK9 (Figure S6C), indicating that the binding of ENB to NEK7 is specific. Because the original function of NEK7 is to mediate mitosis to regulate the cell cycle,[53] we treated RAW264.7 cells with ENB and found that it did not affect the cell cycle (Figures S6D and S6E). In addition to the regulation of mitosis, NEK7 is also involved in a variety of physiological and pathological processes, mainly through its kinase activity.[54,55] We incubated ENB with recombinant WT, R121A, or K64M (kinase inactive[56]) mutant NEK7 and found that neither R121A mutation nor ENB treatment affected the kinase activity of NEK7 (Figures S6F and S6G). Together, these results suggest that ENB specifically binds to NEK7 and inhibits NLRP3 inflammasome activation.

ENB inhibits LPS-induced systemic inflammation and MSU-induced peritonitis

Because ENB significantly inhibited activation of the NLRP3 inflammasome *in vitro*, we subsequently explored its inhibitory effect *in vivo*. A previous study has shown that systemic inflammation is induced by LPS in an NLRP3 inflammasome-dependent manner.[57] We pretreated mice with or without ENB before challenge with LPS and found that ENB treatment significantly improved the survival rate of mice and inhibited the production of IL-1β without affecting the release of TNF-α in serum (Figures 5A–5C). We further analyzed the function of the liver and found that ENB treatment diminished hepatic injury, serum aspartate aminotransferase (AST), and alanine aminotransferase (ALT) levels after LPS injection (Figures 5D–5F). In addition to LPS-induced systemic inflammation, we also tested the effect of ENB on MSU-induced peritonitis. The results showed that ENB treatment reduced MSU-induced neutrophil infiltration

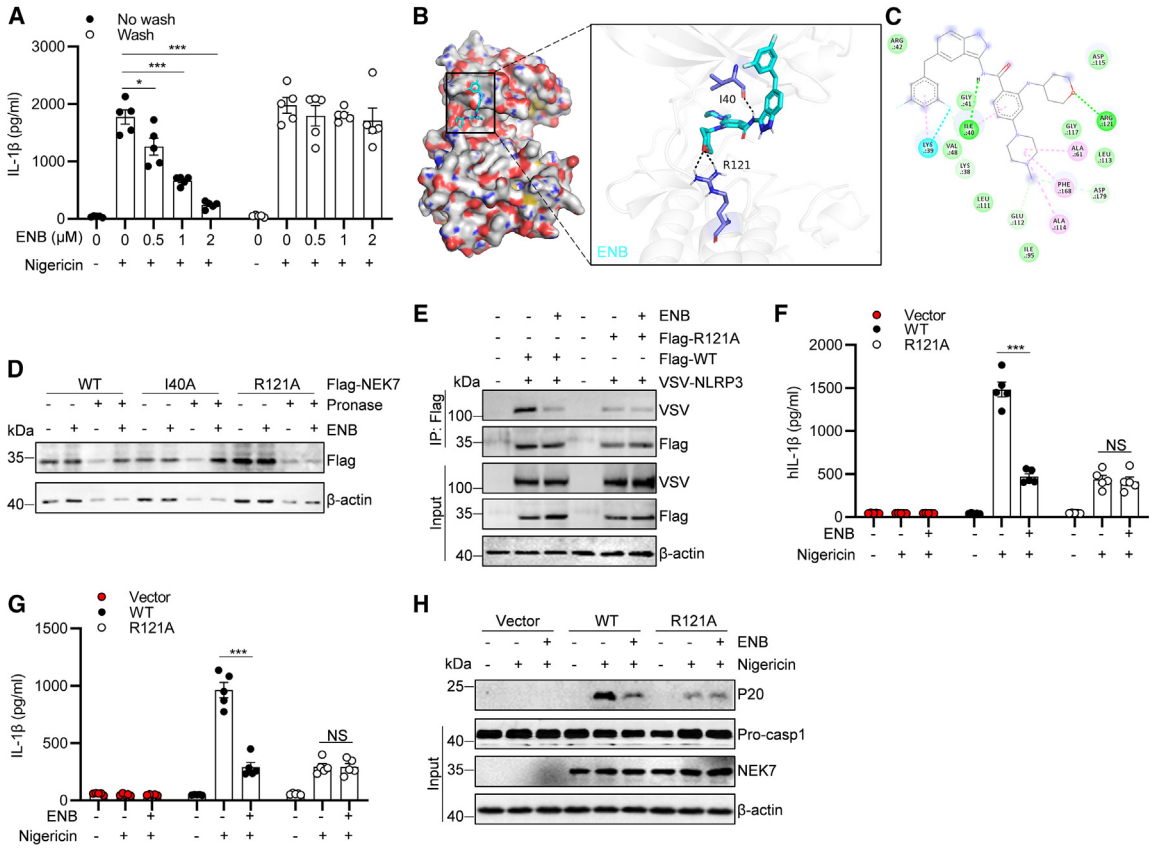

Figure 4. ENB binds to R121 of NEK7

(A) ELISA of IL-1β in SNs from LPS-primed BMDMs treated with various doses of ENB for 15 min and then washed three times and stimulated with 5 μM nigericin for 30 min.

(B) Docking complex of NEK7 with ENB. ENB is shown as sticks and colored light green, NEK7 is showed in cartoon and colored light gray, and key amino acid residues are shown as sticks.

(C) 2D binding mode diagrams of NEK7 and ENB.

(D) DARTS and immunoblot analysis of NEK7 in HEK293T cells transfected with WT, I40A, or R121A mutant FLAG-NEK7 and then treated with 200 μM ENB and pronase (25 ng/μg of protein).

(E) IP and immunoblot analysis of HEK293T cells transfected with VSV-NLRP3, WT, or R121A mutant FLAG-NEK7 plasmids as indicated and treated with 2 μM ENB.

(F) ELISA analysis of IL-1β in SNs from NEK7 knockout THP-1 cells recombined with human WT or R121A mutant NEK7 and then stimulated with 5 μM nigericin for 1 h.

(G) ELISA of IL-1β in SNs from NEK7 knockout iBMDMs recombined with mouse WT or R121A mutant NEK7 and then stimulated with 5 μM nigericin for 2 h.

(H) Immunoblot analysis of P20 in SNs, pro-casp1, and NEK7 in input from NEK7 knockout iBMDMs recombined with mouse WT or R121A mutant NEK7 and then stimulated with 5 μM nigericin for 2 h.

Data are representative of one replicate of five independent experiments and show as mean ± SEM. Statistical analysis was performed using two-way ANOVA (A, F, and G). *$p < 0.05$, ***$p < 0.001$; NS, not significant, $p > 0.05$.

(Figure 5G) and IL-1β production (Figure 5H). Taken together, these results suggest that ENB has therapeutic effects in mouse models of LPS-induced systemic inflammation and MSU-induced peritonitis.

ENB prevents the pathological development of HFD-induced T2D

In addition to the acute inflammatory diseases mentioned above, the NLRP3 inflammasome also contributed to the development of chronic inflammatory diseases, such as T2D.[17,58] Next, we explore the preventive and therapeutic effects of ENB on T2D in a high-fat diet (HFD)-induced mouse model. After feeding C57BL/6J mice an HFD with or without ENB for 16 weeks, we found that ENB treatment significantly prevented mice from gaining weight but did not affect food intake (Figures 6A and S7A). ENB treatment also alleviated the increases in fasting and fed blood glucose concentrations as well as fasting insulin concentrations in HFD-fed mice (Figures 6B, 6C, and S7B). Moreover, by glucose tolerance test (GTT) and insulin tolerance test (ITT), we found that mice treated with ENB exhibited better insulin sensitivity and glucose tolerance compared with the control group (Figures 6D and 6E). In addition, we found that ENB inhibited the weight of liver (Figure S7C). Histological analysis of mouse liver revealed severe hepatic steatosis and lipid

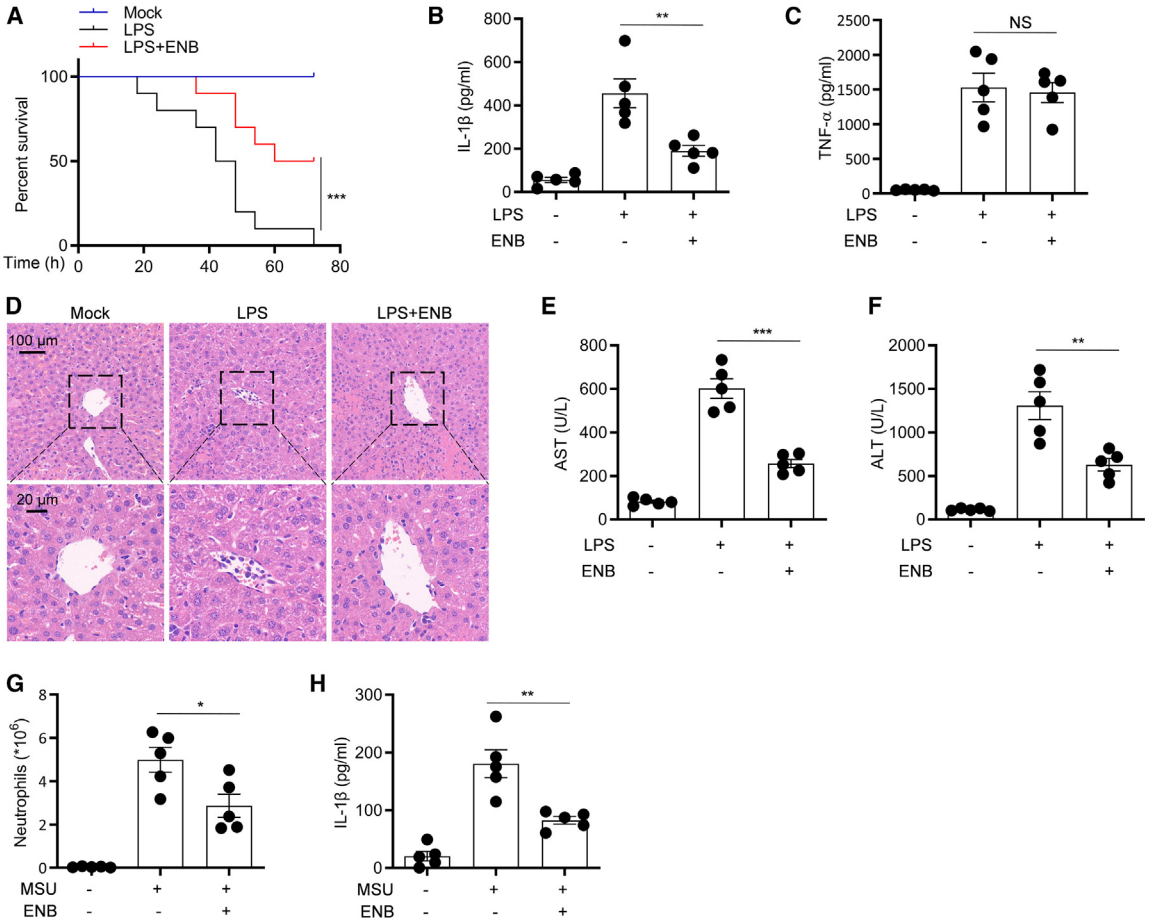

Figure 5. ENB has therapeutic effects in a mouse model of LPS-induced systemic inflammation and MSU-induced peritonitis

(A) Survival analysis of C57BL/6 mice pretreated with vehicle or ENB (10 mg/kg) for 1 h before being intraperitoneally injected with LPS. n = 10 biologically independent mice.

(B and C) ELISA of IL-1β (B) and TNF-α (C) in serum of C57BL/6J mice pretreated with vehicle or ENB for 1 h before being intraperitoneally injected with LPS. N = 5 biologically independent mice.

(D) Hematoxylin and eosin (H&E) staining in liver cross-sections from C57BL/6J mice pretreated with vehicle or ENB for 1 h before being intraperitoneally injected with LPS.

(E and F) Serum AST (E) and ALT (F) levels of C57BL/6J mice pretreated with vehicle or ENB for 1 h before being intraperitoneally injected with LPS. n = 5 biologically independent mice.

(G) Statistical analysis of neutrophil numbers in the peritoneal cavity of C57BL/6J mice pretreated with vehicle or ENB for 1 h before being intraperitoneally injected with MSU. n = 5 biologically independent mice.

(H) ELISA analysis of IL-1β in the peritoneal cavity of C57BL/6J mice pretreated with vehicle or ENB for 1 h before being intraperitoneally injected with MSU. n = 5 biologically independent mice.

Data represent mean ± SEM. Statistical analysis was performed using generalized Wilcoxon test (A) or one-way ANOVA (B, C, and E–H). *$p < 0.05$, **$p < 0.01$, ***$p < 0.001$; NS, $p > 0.05$.

accumulation in HFD-fed mice, which were significantly improved by ENB treatment (Figure S7D). We next explored the alleviating effect of ENB on metainflammation in HFD-fed mice. By measuring IL-1β secretion in serum, liver, and white adipose tissue (WAT) of HFD-fed mice, we found that ENB has a good anti-inflammatory effect (Figures 6F, 6G, and 6I). Moreover, cleavage of caspase-1 and GSDMD in the liver of HFD-fed mice was also suppressed by ENB (Figure 6H). Taken together, these results indicate that ENB treatment prevents the pathological development of HFD-induced T2D by inhibiting NLRP3 inflammasome activation and metainflammation *in vivo*.

ENB has a remarkable therapeutic effect on HFD-induced T2D

We further sought to test whether ENB was effective in reversing HFD-induced T2D in a mouse model after the disease was established. We first fed C57BL/6J mice with HFD for 12 weeks and then treated these mice with ENB for 4 weeks. The results showed that ENB significantly reduced the weight gain and effectively controlled fasting and fed blood glucose concentrations in HFD-fed mice (Figures 7A–7C). Moreover, HFD-fed mice treated with ENB showed better insulin sensitivity and glucose tolerance compared with the control group (Figures 7D and 7E). In addition,

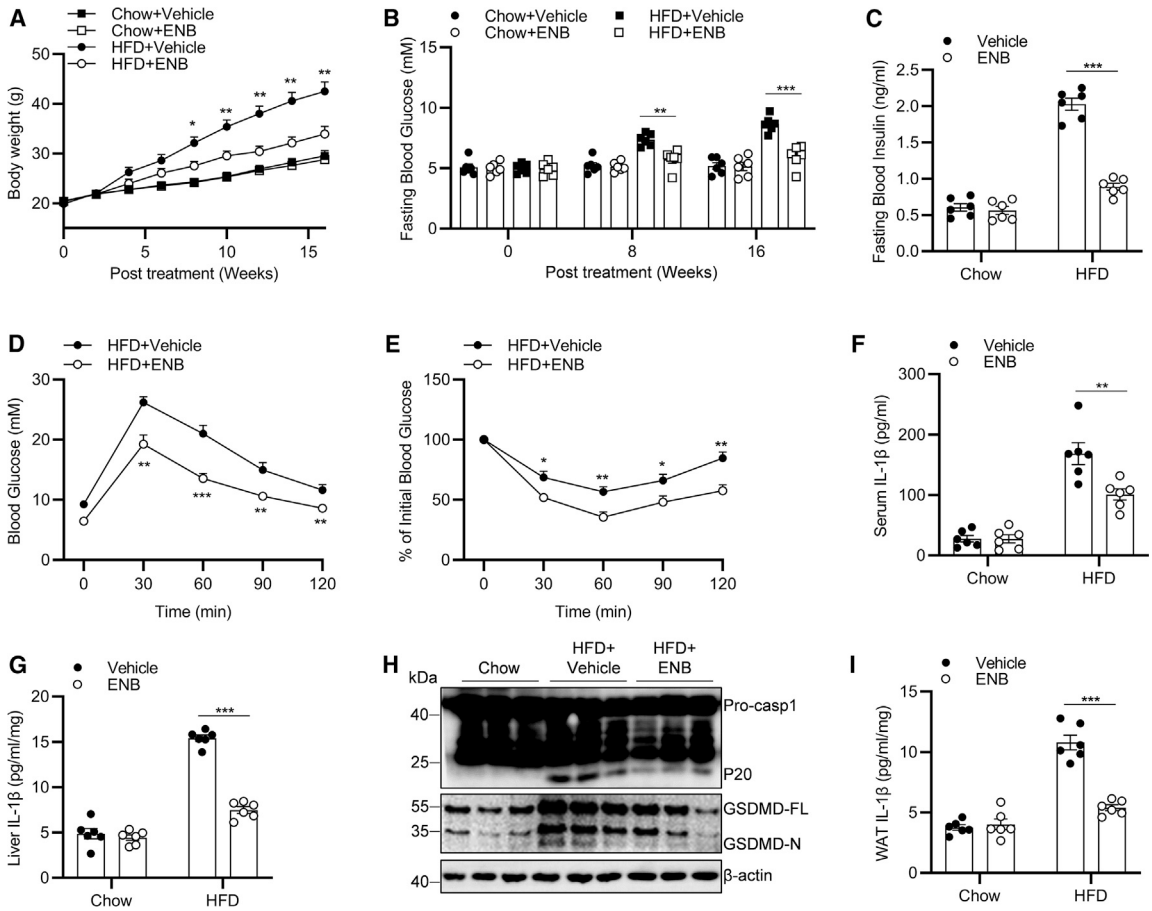

Figure 6. ENB has preventive effects in mouse models of HFD-induced T2D

(A) Body weights of C57BL/6 mice were measured at the indicated time points after initiation of the HFD with or without ENB treatment. n = 6 biologically independent mice.

(B) Fasting blood glucose concentrations of C57BL/6 mice were measured at the indicated time points after initiation of the HFD with or without ENB treatment. n = 6 biologically independent mice.

(C) Fasting blood insulin concentrations of C57BL/6 mice were measured at week 16 after initiation of the HFD with or without ENB treatment. n = 6 biologically independent mice.

(D and E) Glucose tolerance test (GTT) (D) and insulin tolerance test (ITT) (E) of C57BL/6 mice were performed at week 16 after initiation of the HFD with or without ENB treatment. n = 6 biologically independent mice.

(F) ELISA analysis of IL-1β in serum of C57BL/6J mice were measured at week 16 after initiation of the HFD with or without ENB treatment. n = 6 biologically independent mice.

(G) ELISA of IL-1β in liver cultured SNs of C57BL/6 mice at week 16 after initiation of the HFD with or without ENB treatment. n = 6 biologically independent mice.

(H) Immunoblot analysis of P20 and GSDMD in liver of C57BL/6 mice at week 16 after initiation of the HFD with or without ENB treatment.

(I) ELISA of IL-1β in white adipose tissue (WAT) culture SNs of C57BL/6 mice at week 16 after initiation of the HFD with or without ENB treatment. n = 6 biologically independent mice. Data represent mean ± SEM. Statistical analysis was performed using two-way ANOVA (A–G and I). *p < 0.05, **p < 0.01, ***p < 0.001.

we detected IL-1β secretion in serum, liver, and white adipose tissue (WAT) of HFD-fed mice and found that ENB effectively relieved metabolic inflammation (Figures 7F, 7H, and 7I). Histological analysis of mouse liver revealed that ENB significantly improved HFD-induced hepatic steatosis (Figure 7G). Thus, our results demonstrate that ENB has a remarkable therapeutic effect on HFD-induced T2D.

DISCUSSION

In this study, we identified ENB, an FDA-approved clinical anti-cancer agent, as a target inhibitor of NEK7 to restrain NLRP3 inflammasome activation and relieve associated inflammatory diseases, including LPS-induced systemic inflammation, MSU-induced peritonitis, and HFD-induced T2DM in mouse models, suggesting that ENB may serve as a potential candidate drug for the treatment of NLRP3 inflammasome-related diseases.

Abnormal activation of the NLRP3 inflammasome is involved in the pathogenesis of multiple human diseases, including peritonitis, atherosclerosis, T2D, EAE, and neurodegenerative disease.[14–17] Therefore, the NLRP3 inflammasome is a promising drug target for the treatment of inflammatory diseases. Our clinical or FDA-approved kinase inhibitor screening results show that the FDA-approved anti-cancer drug ENB significantly inhibits NLRP3

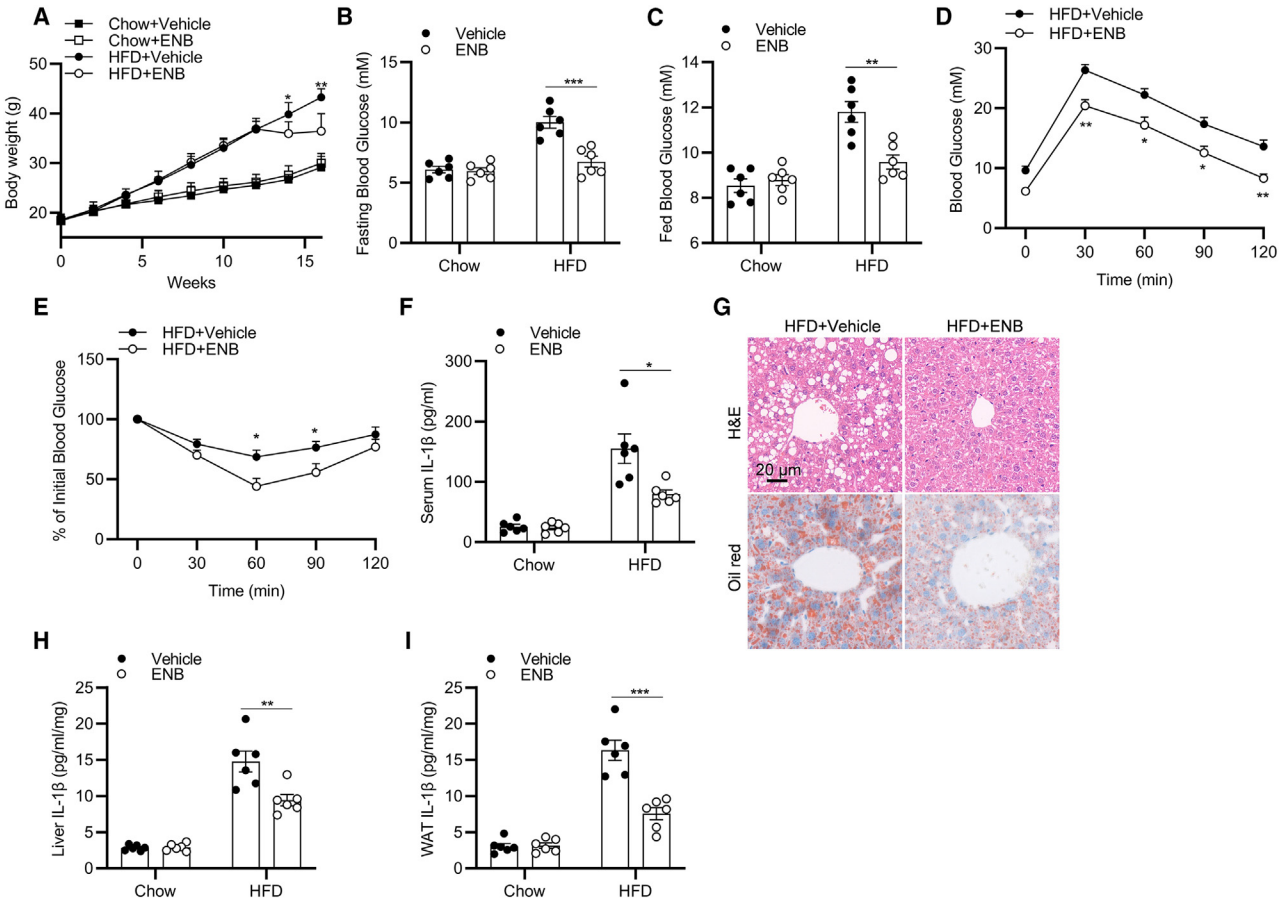

Figure 7. ENB has therapeutic effects in mouse models of HFD-induced T2D

(A) Body weights of C57BL/6 mice were measured at the indicated time points after initiation of the HFD for 12 weeks and then treated with vehicle or ENB for 4 weeks. n = 6 biologically independent mice.

(B and C) Fasting blood glucose (B) and fed blood glucose (C) concentrations of C57BL/6 mice that were first fed with an HFD for 12 weeks and then treated with vehicle or ENB for 4 weeks. n = 6 biologically independent mice.

(D and E) GTT (D) and ITT (E) of C57BL/6 mice that were first fed with an HFD for 12 weeks and then treated with vehicle or ENB for 4 weeks. n = 6 biologically independent mice.

(F) ELISA of IL-1β in serum of C57BL/6J mice that were first fed with an HFD for 12 weeks and then treated with vehicle or ENB for 4 weeks. n = 6 biologically independent mice.

(G) Representative H&E and oil red O staining of liver sections of C57BL/6J mice that were first fed with an HFD for 12 weeks and then treated with vehicle or ENB for 4 weeks.

(H and I) ELISA analysis of IL-1β in liver (H) and WAT (I) culture SNs of C57BL/6 mice that were first fed with an HFD for 12 weeks and then treated with vehicle or ENB for 4 weeks. n = 6 biologically independent mice.

Data represent mean ± SEM. Statistical analysis was performed using two-way ANOVA (A–F, H, and I). *p < 0.05, **p < 0.01, ***p < 0.001.

inflammasome activation at the submicromolar level with an IC_{50} value of 0.88 μM but had no inhibitory effect on the activation of other inflammasomes, indicating that ENB specifically targets the NLRP3 inflammasome. Previous studies have shown that NLRP3 inflammasome activation requires two steps; namely, priming and activation.[59] Our results demonstrate that ENB did not affect the production of IL-6 and TNF-α, indicating that ENB acts downstream of priming signaling. Moreover, ENB had also no effect on potassium and chloride efflux, mitochondrial damage, or ROS production, several critical upstream events for NLRP3 inflammasome activation. Further study revealed that ENB specifically blocked endogenous and exogenous NLRP3-NEK7 interaction, suggesting that it might inhibit NLRP3 inflammasome assembly and activation by directly target NLRP3 or NEK7.

As a key component of the inflammasome, NEK7 is also a potential therapeutic target for NLRP3-related diseases.[60] Several inhibitors, such as manoalide, oridonin, and RRx-001 and its analog have been reported previously to bind to NLRP3 to block its interaction with NEK7.[20,49,61,62] In this study, our results demonstrated that the FDA-approved clinical anti-cancer agent ENB directly binds to NEK7 at R121, a key residue located at the interaction interface between NEK7 and NLRP3,[8] to significantly inhibit NLRP3-NEK7 interaction and inflammasome activation.

Thus, our results provide evidence showing that ENB could be used as a candidate drug to control NLRP3 inflammasome activation by targeting NEK7.

ENB is a multikinase inhibitor with multiple targets, including NTRK, ROS1 and ALK.[31] However, in this study, we confirmed that the inhibitory effect of ENB on the NLRP3 inflammasome does not depend on these targets but on NEK7. NEK7 is highly homologous to two other members of the NEK family, NEK6 and NEK9.[63] To assess the potential off-target effects of ENB, we explored the binding specificity of ENB to NEK7 and found that ENB only interacted with NEK7 but not NEK6 and NEK9. In addition, because NEK7 is a serine/threonine kinase implicated previously in mitosis,[53] we tested the effect of ENB on the cell cycle and found that it did not affect the cell cycle. Furthermore, NEK7 is involved in multiple cellular processes mainly through its kinase activity. We performed *in vitro* kinase activity assays with recombinant NEK7 proteins and found that ENB did not affect the kinase activity of NEK7, indicating that ENB-specific targeting binds to NEK7 to inhibit NLRP3 inflammasome without off-target effects.

ENB is an anti-cancer drug approved by the FDA for the treatment of multiple solid tumors and NSCLC; it has a highly safety profile and is well tolerated by almost all patients without cumulative toxicity at doses up to 600 mg orally once a day continuously for 3 months.[34] Our results demonstrate that ENB has a significant therapeutic effect in multiple mouse models of NLRP3 inflammasome-driven diseases, including LPS-induced systemic inflammation and MSU-induced peritonitis. Moreover, ENB also has good preventive and therapeutic effects on T2D, even at drug concentrations as low as 1 mg/kg. However, the concentration of ENB needs to reach 10 mg/kg to show better efficacy in cancer treatment,[64,65] suggesting that ENB may be a preferential treatment for chronic inflammatory diseases. The pharmacokinetics study of ENB showed that the average plasma concentration of ENB could reach 1.3 μM after 1 mg/kg administration,[64] which was sufficient to inhibit inflammasome activation. Indeed, our results also demonstrated that ENB significantly inhibited secretion of the pro-inflammatory cytokine IL-1β in serum, liver, and WAT of HFD-fed mice.

The NLRP3 inflammasome has been found to be involved in the occurrence and development of multiple inflammatory diseases, including EAE, atherosclerosis and Alzheimer's disease (AD). However, it is still unclear whether ENB has a therapeutic effect on those inflammasome-driven diseases; this needs to be studied further. ENB is a therapeutic drug approved by the FDA with high clinical safety and excellent anti-inflammasome activity *in vitro* and *in vivo*. Therefore, ENB is a promising clinical drug for the treatment of NLRP3 inflammasome-driven diseases.

Limitations of the study

In this study, although we revealed that ENB inhibited NLRP3 inflammasome activation *in vitro* and *in vivo*, because of the limited availability of primary human cells or a relevant human model, our results are based solely on cell experiments and mouse models. Therefore, its clinical application needs to be explored further. In addition, we demonstrated that the inhibitory effect of the NLRP3 inflammasome by ENB is independent of NTRK, ROS1, and ALK *in vitro*, but whether these targets are involved in the disease process *in vivo* remains to be explored. Furthermore, the NLRP3 inflammasome has also been reported to affect tumor initiation and progression, but whether the inhibitory effect of ENB on tumor growth is dependent on NEK7 remains unclear.

STAR★METHODS

Detailed methods are provided in the online version of this paper and include the following:

- KEY RESOURCES TABLE
- RESOURCE AVAILABILITY
  - Lead contact
  - Materials availability
  - Data and code availability
- EXPERIMENTAL MODEL AND STUDY PARTICIPANT DETAILS
  - Mice
  - Cell lines
  - Primary human PBMCs culture
- METHOD DETAILS
  - Inflammasome activation assays
  - ASC oligomerization assay
  - siRNA interference
  - Quantitative real-time PCR
  - Confocal microscopy
  - Intracellular potassium assay
  - Intracellular chloride assay
  - Immunoprecipitation
  - Drug affinity responsive target stability (DARTS) assay
  - Cellular thermal shift assay (CETSA)
  - *In vitro* kinase activity assay
  - LPS-induced systemic inflammation
  - MSU-induced peritonitis
  - High-fat diet (HFD) and ENB treatment
  - Glucose tolerance or insulin tolerance test
  - Histological analysis
- QUANTIFICATION AND STATISTICAL ANALYSIS

SUPPLEMENTAL INFORMATION

Supplemental information can be found online at https://doi.org/10.1016/j.xcrm.2023.101310.

ACKNOWLEDGMENTS

This research was supported by the National Natural Science Foundation of China (82202038) and the Natural Science Foundation of Jiangsu Province (BK20221085). BioRender was used to make the graphical abstract.

AUTHOR CONTRIBUTIONS

Conceptualization and experimental design, X.J., D.L., and Y.H.; experiment progress and data analysis, X.J., D.L., X.Z. X.L., and Q.H.; manuscript writing and editing, X.J., D.L., and Y.H.; funding acquisition, Y.H.

DECLARATION OF INTERESTS

The authors declare no competing interests.

INCLUSION AND DIVERSITY

We support inclusive, diverse, and equitable conduct of research.

Received: April 17, 2023
Revised: October 5, 2023
Accepted: November 13, 2023
Published: December 19, 2023

REFERENCES

1. Jin, X., Zhou, R., and Huang, Y. (2022). Role of inflammasomes in HIV-1 infection and treatment. Trends Mol. Med. *28*, 421–434.
2. Guo, H., Callaway, J.B., and Ting, J.P.Y. (2015). Inflammasomes: mechanism of action, role in disease, and therapeutics. Nat. Med. *21*, 677–687.
3. Huang, Y., Wang, H., Hao, Y., Lin, H., Dong, M., Ye, J., Song, L., Wang, Y., Li, Q., Shan, B., et al. (2020). Myeloid PTEN promotes chemotherapy-induced NLRP3-inflammasome activation and antitumour immunity. Nat. Cell Biol. *22*, 716–727.
4. Heneka, M.T., Kummer, M.P., Stutz, A., Delekate, A., Schwartz, S., Vieira-Saecker, A., Griep, A., Axt, D., Remus, A., Tzeng, T.C., et al. (2013). NLRP3 is activated in Alzheimer's disease and contributes to pathology in APP/PS1 mice. Nature *493*, 674–678.
5. Martinon, F., Pétrilli, V., Mayor, A., Tardivel, A., and Tschopp, J. (2006). Gout-associated uric acid crystals activate the NALP3 inflammasome. Nature *440*, 237–241.
6. Wang, X., Jiang, W., Yan, Y., Gong, T., Han, J., Tian, Z., and Zhou, R. (2014). RNA viruses promote activation of the NLRP3 inflammasome through a RIP1-RIP3-DRP1 signaling pathway. Nat. Immunol. *15*, 1126–1133.
7. He, Y., Zeng, M.Y., Yang, D., Motro, B., and Núñez, G. (2016). NEK7 is an essential mediator of NLRP3 activation downstream of potassium efflux. Nature *530*, 354–357.
8. Sharif, H., Wang, L., Wang, W.L., Magupalli, V.G., Andreeva, L., Qiao, Q., Hauenstein, A.V., Wu, Z., Núñez, G., Mao, Y., and Wu, H. (2019). Structural mechanism for NEK7-licensed activation of NLRP3 inflammasome. Nature *570*, 338–343.
9. Xu, W., and Huang, Y. (2022). Regulation of Inflammatory Cell Death by Phosphorylation. Front. Immunol. *13*, 851169.
10. Kayagaki, N., Stowe, I.B., Lee, B.L., O'Rourke, K., Anderson, K., Warming, S., Cuellar, T., Haley, B., Roose-Girma, M., Phung, Q.T., et al. (2015). Caspase-11 cleaves gasdermin D for non-canonical inflammasome signalling. Nature *526*, 666–671.
11. He, W.T., Wan, H., Hu, L., Chen, P., Wang, X., Huang, Z., Yang, Z.H., Zhong, C.Q., and Han, J. (2015). Gasdermin D is an executor of pyroptosis and required for interleukin-1beta secretion. Cell Res. *25*, 1285–1298.
12. Shi, J., Zhao, Y., Wang, K., Shi, X., Wang, Y., Huang, H., Zhuang, Y., Cai, T., Wang, F., and Shao, F. (2015). Cleavage of GSDMD by inflammatory caspases determines pyroptotic cell death. Nature *526*, 660–665.
13. Huang, Y., Xu, W., and Zhou, R. (2021). NLRP3 inflammasome activation and cell death. Cell. Mol. Immunol. *18*, 2114–2127.
14. Strowig, T., Henao-Mejia, J., Elinav, E., and Flavell, R. (2012). Inflammasomes in health and disease. Nature *481*, 278–286.
15. Duewell, P., Kono, H., Rayner, K.J., Sirois, C.M., Vladimer, G., Bauernfeind, F.G., Abela, G.S., Franchi, L., Nuñez, G., Schnurr, M., et al. (2010). NLRP3 inflammasomes are required for atherogenesis and activated by cholesterol crystals. Nature *464*, 1357–1361.
16. Inoue, M., Williams, K.L., Gunn, M.D., and Shinohara, M.L. (2012). NLRP3 inflammasome induces chemotactic immune cell migration to the CNS in experimental autoimmune encephalomyelitis. Proc. Natl. Acad. Sci. USA *109*, 10480–10485.
17. Zhou, R., Tardivel, A., Thorens, B., Choi, I., and Tschopp, J. (2010). Thioredoxin-interacting protein links oxidative stress to inflammasome activation. Nat. Immunol. *11*, 136–140.
18. Zahid, A., Li, B., Kombe, A.J.K., Jin, T., and Tao, J. (2019). Pharmacological Inhibitors of the NLRP3 Inflammasome. Front. Immunol. *10*, 2538.
19. Huang, Y., Guo, Y., Zhou, Y., Huang, Q., Ru, Y., Luo, Y., and Xu, W. (2023). Tivantinib alleviates inflammatory diseases by directly targeting NLRP3. iScience *26*, 106062.
20. He, H., Jiang, H., Chen, Y., Ye, J., Wang, A., Wang, C., Liu, Q., Liang, G., Deng, X., Jiang, W., and Zhou, R. (2018). Oridonin is a covalent NLRP3 inhibitor with strong anti-inflammasome activity. Nat. Commun. *9*, 2550.
21. Huang, Y., Jiang, H., Chen, Y., Wang, X., Yang, Y., Tao, J., Deng, X., Liang, G., Zhang, H., Jiang, W., and Zhou, R. (2018). Tranilast directly targets NLRP3 to treat inflammasome-driven diseases. EMBO Mol. Med. *10*, e8689.
22. Coll, R.C., Hill, J.R., Day, C.J., Zamoshnikova, A., Boucher, D., Massey, N.L., Chitty, J.L., Fraser, J.A., Jennings, M.P., Robertson, A.A.B., and Schroder, K. (2019). MCC950 directly targets the NLRP3 ATP-hydrolysis motif for inflammasome inhibition. Nat. Chem. Biol. *15*, 556–559.
23. Coll, R.C., Robertson, A.A.B., Chae, J.J., Higgins, S.C., Muñoz-Planillo, R., Inserra, M.C., Vetter, I., Dungan, L.S., Monks, B.G., Stutz, A., et al. (2015). A small-molecule inhibitor of the NLRP3 inflammasome for the treatment of inflammatory diseases. Nat. Med. *21*, 248–255.
24. Jiang, H., He, H., Chen, Y., Huang, W., Cheng, J., Ye, J., Wang, A., Tao, J., Wang, C., Liu, Q., et al. (2017). Identification of a selective and direct NLRP3 inhibitor to treat inflammatory disorders. J. Exp. Med. *214*, 3219–3238.
25. Lipinska, K., Malone, K.E., Moerland, M., and Kluft, C. (2014). Applying caspase-1 inhibitors for inflammasome assays in human whole blood. J. Immunol. Methods *411*, 66–69.
26. Wu, J., Lan, Y., Shi, X., Huang, W., Li, S., Zhang, J., Wang, H., Wang, F., and Meng, X. (2022). Sennoside A is a novel inhibitor targeting caspase-1. Food Funct. *13*, 9782–9795.
27. Pan, L., Tang, W.D., Wang, K., Fang, Q.F., Liu, M.R., Wu, Z.X., Wang, Y., Cui, S.L., Hu, G., Hou, T.J., et al. (2022). Novel Caspase-1 inhibitor CZL80 improves neurological function in mice after progressive ischemic stroke within a long therapeutic time-window. Acta Pharmacol. Sin. *43*, 2817–2827.
28. Rathkey, J.K., Zhao, J., Liu, Z., Chen, Y., Yang, J., Kondolf, H.C., Benson, B.L., Chirieleison, S.M., Huang, A.Y., Dubyak, G.R., et al. (2018). Chemical disruption of the pyroptotic pore-forming protein gasdermin D inhibits inflammatory cell death and sepsis. Sci. Immunol. *3*, eaat2738.
29. Humphries, F., Shmuel-Galia, L., Ketelut-Carneiro, N., Li, S., Wang, B., Nemmara, V.V., Wilson, R., Jiang, Z., Khalighinejad, F., Muneeruddin, K., et al. (2020). Succination inactivates gasdermin D and blocks pyroptosis. Science *369*, 1633–1637.
30. Hu, J.J., Liu, X., Xia, S., Zhang, Z., Zhang, Y., Zhao, J., Ruan, J., Luo, X., Lou, X., Bai, Y., et al. (2020). FDA-approved disulfiram inhibits pyroptosis by blocking gasdermin D pore formation. Nat. Immunol. *21*, 736–745.
31. Liu, D., Offin, M., Harnicar, S., Li, B.T., and Drilon, A. (2018). Entrectinib: an orally available, selective tyrosine kinase inhibitor for the treatment of NTRK, ROS1, and ALK fusion-positive solid tumors. Therapeut. Clin. Risk Manag. *14*, 1247–1252.
32. Marcus, L., Donoghue, M., Aungst, S., Myers, C.E., Helms, W.S., Shen, G., Zhao, H., Stephens, O., Keegan, P., and Pazdur, R. (2021). FDA Approval Summary: Entrectinib for the Treatment of NTRK gene Fusion Solid Tumors. Clin. Cancer Res. *27*, 928–932.
33. Drilon, A., Chiu, C.H., Fan, Y., Cho, B.C., Lu, S., Ahn, M.J., Krebs, M.G., Liu, S.V., John, T., Otterson, G.A., et al. (2022). Long-Term Efficacy and Safety of Entrectinib in ROS1 Fusion-Positive NSCLC. JTO Clin. Res. Rep. *3*, 100332.
34. Jiang, Q., Li, M., Li, H., and Chen, L. (2022). Entrectinib, a new multi-target inhibitor for cancer therapy. Biomed. Pharmacother. *150*, 112974.

35. Groß, C.J., Mishra, R., Schneider, K.S., Médard, G., Wettmarshausen, J., Dittlein, D.C., Shi, H., Gorka, O., Koenig, P.A., Fromm, S., et al. (2016). K(+) Efflux-Independent NLRP3 Inflammasome Activation by Small Molecules Targeting Mitochondria. Immunity *45*, 761–773.

36. Eisenbarth, S.C., Colegio, O.R., O'Connor, W., Sutterwala, F.S., and Flavell, R.A. (2008). Crucial role for the Nalp3 inflammasome in the immunostimulatory properties of aluminium adjuvants. Nature *453*, 1122–1126.

37. Franchi, L., and Núñez, G. (2008). The Nlrp3 inflammasome is critical for aluminium hydroxide-mediated IL-1beta secretion but dispensable for adjuvant activity. Eur. J. Immunol. *38*, 2085–2089.

38. Hornung, V., Bauernfeind, F., Halle, A., Samstad, E.O., Kono, H., Rock, K.L., Fitzgerald, K.A., and Latz, E. (2008). Silica crystals and aluminum salts activate the NALP3 inflammasome through phagosomal destabilization. Nat. Immunol. *9*, 847–856.

39. Kayagaki, N., Wong, M.T., Stowe, I.B., Ramani, S.R., Gonzalez, L.C., Akashi-Takamura, S., Miyake, K., Zhang, J., Lee, W.P., Muszyński, A., et al. (2013). Noncanonical inflammasome activation by intracellular LPS independent of TLR4. Science *341*, 1246–1249.

40. Kayagaki, N., Warming, S., Lamkanfi, M., Vande Walle, L., Louie, S., Dong, J., Newton, K., Qu, Y., Liu, J., Heldens, S., et al. (2011). Non-canonical inflammasome activation targets caspase-11. Nature *479*, 117–121.

41. Fernandes-Alnemri, T., Yu, J.W., Datta, P., Wu, J., and Alnemri, E.S. (2009). AIM2 activates the inflammasome and cell death in response to cytoplasmic DNA. Nature *458*, 509–513.

42. Hornung, V., Ablasser, A., Charrel-Dennis, M., Bauernfeind, F., Horvath, G., Caffrey, D.R., Latz, E., and Fitzgerald, K.A. (2009). AIM2 recognizes cytosolic dsDNA and forms a caspase-1-activating inflammasome with ASC. Nature *458*, 514–518.

43. Broz, P., von Moltke, J., Jones, J.W., Vance, R.E., and Monack, D.M. (2010). Differential requirement for Caspase-1 autoproteolysis in pathogen-induced cell death and cytokine processing. Cell Host Microbe *8*, 471–483.

44. Xu, H., Yang, J., Gao, W., Li, L., Li, P., Zhang, L., Gong, Y.N., Peng, X., Xi, J.J., Chen, S., et al. (2014). Innate immune sensing of bacterial modifications of Rho GTPases by the Pyrin inflammasome. Nature *513*, 237–241.

45. Hara, H., Seregin, S.S., Yang, D., Fukase, K., Chamaillard, M., Alnemri, E.S., Inohara, N., Chen, G.Y., and Núñez, G. (2018). The NLRP6 Inflammasome Recognizes Lipoteichoic Acid and Regulates Gram-Positive Pathogen Infection. Cell *175*, 1651–1664.e14.

46. Youm, Y.H., Nguyen, K.Y., Grant, R.W., Goldberg, E.L., Bodogai, M., Kim, D., D'Agostino, D., Planavsky, N., Lupfer, C., Kanneganti, T.D., et al. (2015). The ketone metabolite beta-hydroxybutyrate blocks NLRP3 inflammasome-mediated inflammatory disease. Nat. Med. *21*, 263–269.

47. Mangan, M.S.J., Olhava, E.J., Roush, W.R., Seidel, H.M., Glick, G.D., and Latz, E. (2018). Targeting the NLRP3 inflammasome in inflammatory diseases. Nat. Rev. Drug Discov. *17*, 588–606.

48. Swanson, K.V., Deng, M., and Ting, J.P.Y. (2019). The NLRP3 inflammasome: molecular activation and regulation to therapeutics. Nat. Rev. Immunol. *19*, 477–489.

49. Chen, Y., He, H., Lin, B., Chen, Y., Deng, X., Jiang, W., and Zhou, R. (2021). RRx-001 ameliorates inflammatory diseases by acting as a potent covalent NLRP3 inhibitor. Cell. Mol. Immunol. *18*, 1425–1436.

50. Jafari, R., Almqvist, H., Axelsson, H., Ignatushchenko, M., Lundbäck, T., Nordlund, P., and Martinez Molina, D. (2014). The cellular thermal shift assay for evaluating drug target interactions in cells. Nat. Protoc. *9*, 2100–2122.

51. Schmacke, N.A., O'Duill, F., Gaidt, M.M., Szymanska, I., Kamper, J.M., Schmid-Burgk, J.L., Madler, S.C., Mackens-Kiani, T., Kozaki, T., Chauhan, D., et al. (2022). IKKbeta primes inflammasome formation by recruiting NLRP3 to the trans-Golgi network. Immunity *55*, 2271–2284 e2277.

52. Belham, C., Roig, J., Caldwell, J.A., Aoyama, Y., Kemp, B.E., Comb, M., and Avruch, J. (2003). A mitotic cascade of NIMA family kinases. Nercc1/Nek9 activates the Nek6 and Nek7 kinases. J. Biol. Chem. *278*, 34897–34909.

53. Yissachar, N., Salem, H., Tennenbaum, T., and Motro, B. (2006). Nek7 kinase is enriched at the centrosome, and is required for proper spindle assembly and mitotic progression. FEBS Lett. *580*, 6489–6495.

54. Sun, Z., Gong, W., Zhang, Y., and Jia, Z. (2020). Physiological and Pathological Roles of Mammalian NEK7. Front. Physiol. *11*, 606996.

55. Tan, R., Nakajima, S., Wang, Q., Sun, H., Xue, J., Wu, J., Hellwig, S., Zeng, X., Yates, N.A., Smithgall, T.E., et al. (2017). Nek7 Protects Telomeres from Oxidative DNA Damage by Phosphorylation and Stabilization of TRF1. Mol. Cell *65*, 818–831.e5.

56. O'Regan, L., and Fry, A.M. (2009). The Nek6 and Nek7 protein kinases are required for robust mitotic spindle formation and cytokinesis. Mol. Cell Biol. *29*, 3975–3990.

57. Wang, Z., Zhang, S., Xiao, Y., Zhang, W., Wu, S., Qin, T., Yue, Y., Qian, W., and Li, L. (2020). NLRP3 Inflammasome and Inflammatory Diseases. Oxid. Med. Cell. Longev. *2020*, 4063562.

58. Masters, S.L., Dunne, A., Subramanian, S.L., Hull, R.L., Tannahill, G.M., Sharp, F.A., Becker, C., Franchi, L., Yoshihara, E., Chen, Z., et al. (2010). Activation of the NLRP3 inflammasome by islet amyloid polypeptide provides a mechanism for enhanced IL-1beta in type 2 diabetes. Nat. Immunol. *11*, 897–904.

59. Kelley, N., Jeltema, D., Duan, Y., and He, Y. (2019). The NLRP3 Inflammasome: An Overview of Mechanisms of Activation and Regulation. Int. J. Mol. Sci. *20*, 3328.

60. Liu, G., Chen, X., Wang, Q., and Yuan, L. (2020). NEK7: a potential therapy target for NLRP3-related diseases. Biosci. Trends *14*, 74–82.

61. Lin, H., Yang, M., Li, C., Lin, B., Deng, X., He, H., and Zhou, R. (2022). An RRx-001 Analogue With Potent Anti-NLRP3 Inflammasome Activity but Without High-Energy Nitro Functional Groups. Front. Pharmacol. *13*, 822833.

62. Li, C., Lin, H., He, H., Ma, M., Jiang, W., and Zhou, R. (2022). Inhibition of the NLRP3 Inflammasome Activation by Manoalide Ameliorates Experimental Autoimmune Encephalomyelitis Pathogenesis. Front. Cell Dev. Biol. *10*, 822236.

63. Belham, C., Roig, J., Caldwell, J.A., Aoyama, Y., Kemp, B.E., Comb, M., and Avruch, J. (2003). A Mitotic Cascade of NIMA Family Kinases. J. Biol. Chem. *278*, 34897–34909.

64. Fischer, H., Ullah, M., de la Cruz, C.C., Hunsaker, T., Senn, C., Wirz, T., Wagner, B., Draganov, D., Vazvaei, F., Donzelli, M., et al. (2020). Entrectinib, a TRK/ROS1 inhibitor with anti-CNS tumor activity: differentiation from other inhibitors in its class due to weak interaction with P-glycoprotein. Neuro Oncol. *22*, 819–829.

65. Frampton, J.E. (2021). Entrectinib: A Review in NTRK+ Solid Tumours and ROS1+ NSCLC. Drugs *81*, 697–708.

66. Shi, H., Wang, Y., Li, X., Zhan, X., Tang, M., Fina, M., Su, L., Pratt, D., Bu, C.H., Hildebrand, S., et al. (2016). NLRP3 activation and mitosis are mutually exclusive events coordinated by NEK7, a new inflammasome component. Nat. Immunol. *17*, 250–258.

67. Liu, D., and Huang, Y. (2023). Protocol for in vivo and in vitro activation of NLRP3 inflammasome in mice using monosodium urate. STAR Protoc. *4*, 102554.

STAR★METHODS

KEY RESOURCES TABLE

REAGENT or RESOURCE	SOURCE	IDENTIFIER
Antibodies		
Anti-mouse IL-1β	R&D Systems	Cat#AF-401-NA; RRID:AB_416684
Anti-mouse caspase-1	Adipogen	Cat#AG-20B-0042; RRID:AB_2490248
Anti-human IL-1β	Proteintech	Cat#60136-1-Ig; RRID:AB_10597543
Anti-human caspase-1	Cell Signaling Technology	Cat#2225; RRID:AB_2243894
Anti-NLRP3	Adipogen	Cat#AG-20B-0014; RRID:AB_2885199
Anti-β-actin	Abmart	Cat#P30002; RRID:AB_2222847
Anti-ASC	Cell Signaling Technology	Cat#67824; RRID:AB_2799736
Anti-NEK7	Santa Cruz	Cat#SC-50756; RRID:AB_2235871
Anti-NEK6	Abcam	Cat#ab133494; RRID:AB_11155676
Anti-NEK9	Abcam	Cat# ab18332, RRID:AB_444424
Anti-GSDMD	Abcam	Cat#ab219800; RRID:AB_2888940
Anti-VSV	Sigma	Cat#V4888; RRID:AB_261872
Anti-Flag	Sigma	Cat#F2555; RRID:AB_796202
Chemicals, peptides, and recombinant proteins		
Entrectinib	TargetMol	Cat#T3678
Repotrectinib	TargetMol	Cat#T4071
Belizatinib	TargetMol	Cat#T4257
Larotrectinib	TargetMol	Cat#T5995
Val-boroPro	TargetMol	Cat#T37861
MSU	Sigma	Cat#69-93-2
ATP	Sigma	Cat#34369-07-8
PMA (phorbol-12-myristate-13-acetate)	Sigma	Cat#P8139
Poly (dA:dT)	Sigma	Cat#86828-69-5
Protein G agarose	Sigma	Cat#P7700
Propidium iodide (PI)	Sigma	Cat#P4170
β-hydroxybutyrate (BHB)	Sigma	Cat#52017
Pronase	Sigma	Cat#P5147
Imiquimod	MedChemExpress	Cat#HY-B0180
Nigericin	MedChemExpress	Cat#HY-127019
MCC950	MedChemExpress	Cat#HY-12815
CY-09	MedChemExpress	Cat#HY-103666
Tranilast	MedChemExpress	Cat#HY-B0195
Tivantinib	MedChemExpress	Cat#HY-50686
β-Estradiol	MedChemExpress	Cat#HY-B0141
Alum	Thermo Fisher Scientific	Cat#77161
Mitotracker	Thermo Fisher Scientific	Cat#M7512
Pam3CSK4	Invivogen	Cat#tlrl-pms
LPS	Invivogen	Cat#tlrl-peklps
MitoSOX	Invitrogen	Cat#M36008
DAPI	Invitrogen	Cat#D21490
MQAE	Invitrogen	Cat#162558-52-3
Lipofectamine 2000	Invitrogen	Cat#11668019
SiO_2	InvivoGen	Cat#tlrl-sio-2

(*Continued on next page*)

Continued

REAGENT or RESOURCE	SOURCE	IDENTIFIER
Mouse M-CSF	Novoprotein	Cat#CB34
Human M-CSF	Novoprotein	Cat#C417
Human IL-3	Novoprotein	Cat#CF63
Critical commercial assays		
LDH Cytotoxicity Assay Kit	Beyotime	Cat#C0017
Mouse IL-1β ELISA kit	R&D	Cat#DY401
Mouse TNF-alpha ELISA kit	R&D	Cat#DY410
Mouse IL-6 ELISA kit	R&D	Cat#DY406
Human IL-1β ELISA kit	R&D	Cat#DY201
Experimental models: Cell lines		
HEK-293T	ATCC	ATCC Cat#CRL-3216
THP-1	ATCC	ATCC Cat#TIB-202
RAW 264.7	ATCC	ATCC Cat#TIB-71
Experimental models: Organisms/strains		
C57BL/6J	Jackson Laboratory	000664
Oligonucleotides		
Mouse ROS1 forward	Sangon	5′TGGTACCTACTA TCCCTGGA’
Mouse ROS1 reverse	Sangon	5′TCCTTTCCCAAG TGAAGGCC’
Mouse Gapdh forward	Sangon	5′GGTGAAGGTCGGTGTGAACG3′
Mouse Gapdh reverse	Sangon	5′CTCGCTCCTGGAAGATGGTG3′
Software and algorithms		
EndNote X8	EndNote Software	https://endnote.com/
Grahpad Prism (v9)	GraphPad Software	https://www.graphpad.com/
ImageJ 1.47v	National Institutes of Health	https://imagej.nih.gov/ij/
BioRender	BioRender software	https://www.biorender.com/

RESOURCE AVAILABILITY

Lead contact

Further information and requests for resources and reagents should be directed to and will be fulfilled by the lead contact, Yi Huang (HY527@ustc.edu.cn).

Materials availability

This study did not generate new unique materials or reagents.

Data and code availability

- All data reported in this paper is available from the lead contact upon request.
- This study does not generate original code.
- Any additional information required to reanalyze the data reported in this work paper is available from the lead contact upon request.

EXPERIMENTAL MODEL AND STUDY PARTICIPANT DETAILS

Mice

The male C57BL/6J mice used in this study were purchased from Model Animal Research Center of Nanjing University. All mice were specific pathogen-free and housed under a 12 h light–dark cycle at 22°C–24°C with unrestricted access to food and water for the duration of the experiment. All animal experiment protocols and procedures were approved by the Ethics Committee of Jiangnan University. The study is compliant with all relevant ethical regulations regarding animal research.

Cell lines

Primary bone marrow-derived macrophages (BMDMs) were derived from C57BL/6 mice and cultured for 4 days in DMEM supplemented with 10% FBS, 1% penicillin/streptomycin (P/S), 1 mM sodium pyruvate, 2 mM L-glutamine and 20 ng/mL recombinant M-CSF. HEK-293T cells were cultured in DMEM supplemented with 10% FBS, 1% penicillin/streptomycin (P/S), 1 mM sodium pyruvate and 2 mM L-glutamine. THP-1 and BLaER1 cells were cultured in RPMI 1640 medium containing 10% FBS and 1% P/S, 1 mM sodium pyruvate and 2 mM L-glutamine. BLaER1 cells were transdifferentiated into monocytes in RPMI 1640 medium containing 10 ng/mL human IL-3, 100 nM β-Estradiol and 20 ng/mL human M-CSF for 5 days. All of the cells were cultured at 37°C under 5% CO2 and routinely tested for mycoplasma contamination.

Primary human PBMCs culture

Human PBMCs were isolated from fresh peripheral blood using Lymphocyte Separation Medium and cultured in RPMI 1640 medium containing 10% FBS, 1% penicillin/streptomycin (P/S), 1 mM sodium pyruvate and 2 mM L-glutamine.

METHOD DETAILS

Inflammasome activation assays

BMDMs were seeded overnight in 12-well plates and the medium was replaced with Opti-MEM supplemented with 1% FBS and 50 ng/mL LPS for 3 h in the following day. The cells were treated with DMSO or inhibitors for 30 min and then stimulated with different inducers, as follows: 5 μM nigericin or 2.5 mM ATP for 30 min; 0.5 μg/mL Clostridium difficile toxin B (TcdB) for 1 h; 15 μg/mL imiquimod for 3 h; 150 μg/mL MSU, transfection 0.5 μg/mL poly (dA:dT) for 4 h; 300 μg/mL Alum or SiO_2 for 6 h; infected with *Salmonella typhimurium* (multiplicity of infection (MOI) = 5) or *Listeria monocytogenes* (MOI = 10) for 1 h, and then 20 μg/mL gentamicin was added to the culture medium and the stimulation was continued for another 3 h. For noncanonical NLRP3 inflammasome activation, BMDMs were primed with 400 ng/mL pam3CSK4 for 4 h and then transfected with 0.5 μg/mL LPS for 16 h through using the Lipofectamine 2000 according to the manufacturer's protocol (Invitrogen). THP-1 cells were differentiated with 100 nM PMA for 4 h and then the media was removed. The THP-1 cells were resuspended in new RPMI 1640 medium and seeded overnight in 12-well plates. In the following day, the medium was replaced with Opti-MEM supplemented with 1% FBS and 200 ng/mL LPS for 3 h. The cells were treated with DMSO or inhibitors for 30 min and then stimulated with 5 μM nigericin for 1 h or 10 μM ValboroPro (VbP) for 24 h. Human PBMCs were treated with DMSO or inhibitors for 30 min and then stimulated with 1 μg/mL LPS for 24 h. Transdifferentiated BLaER1 cells were primed with 1 μg/mL pam3CSK4 for 4 h and then stimulated with 5 μM nigericin for 2 h. Supernatants were analyzed by ELISA kits according to the manufacturer's instructions (R&D Systems) or by immunoblotting. LDH release was measured using the LDH Cytotoxicity Assay Kit (Beyotime).

ASC oligomerization assay

BMDMs were seeded at 1×10^6 cells/ml in 6-well plates and cultured overnight. In the following day, the medium was replaced with Opti-MEM supplemented with 1% FBS and the cells were primed with 50 ng/mL LPS for 3 h. After priming, the cells were treated with DMSO or different doses of ENB for 30 min and then stimulated with 5 μM nigericin for an additional 30 min. Removing the medium and washing the cells with ice-cold PBS, and then lysing the cells on the shaker with ice-cold NP-40 buffer (50 mM Tris, pH 7.8, 1% Nonidet-P40, 50 mM NaCl, 5 mM EDTA and 10% glycerol) for 30 min. Cell lysate was collected and centrifuged at 330 × g for 10 min at 4°C. The pellets were washed in ice-cold PBS for three times and then resuspended in 500 μL ice-cold PBS with 2 mM disuccinimydylsuberate (DSS). The pellets were incubated at room temperature with rotation for 30 min. Samples were centrifuged at 330 × g for 10 min at 4°C and then the cross-linked pellets were dissolved in 30 μL sample buffer for boiling and blotting.

siRNA interference

3×10^5 BMDMs were seeded overnight in 12-well plates and the medium was replaced with Opti-MEM. Then, the cells were transfected with 50 nM siRNA by RNAimax according to the manufacturer's guidelines (Invitrogen). The siRNA was obtained from GE Dharmacon.

Quantitative real-time PCR

Total RNA extraction of BMDMs were isolated by eusing TRIzol reagent (Invitrogen). RNA (1μg) of each sample was used to generate cDNA using the M-MLV Reverse Transcriptase kit (Invitrogen) according to the manufacturer's protocol. Quantitative PCR was performed using the SYBR Green premix (Takara) in a Roche LightCycler 96. GAPDH was used as the reference gene. The sequences of the gene-specific primers used were as follows: Mouse ROS1 forward, TGGTACCTACTATCCCTGGA; Mouse ROS1 reverse, TCCT TTCCCAAGTGAAGGCC; Mouse GAPDH forward, GGTGAAGGTCGGTGTGAACG, Mouse GAPDH reverse, CTCGCTCCTGGAA GATGGTG.

Confocal microscopy

3×10^5 BMDMs were seeded on coverslips overnight in 12-well plates and then the medium was replaced with Opti-MEM supplemented with 1% FBS and 50 ng/mL LPS for 3 h in the following day. The cells were treated with DMSO or indicated inhibitors for

30 min and stimulated with 5 μM nigericin for 30 min, and then stained with 5 μM MitoSOX or 50 nM MitoTracker Red for 30 min. Removing the medium and washing the cells with ice-cold PBS for three times. Fixing the cells with 4% PFA in PBS for 15 min and then washing three times with PBST. DAPI was used to stain nuclei. Confocal microscopy images were acquired using a Zeiss LSM800 equipped with 63× oil immersion objective. All images were analyzed with ImageJ 1.47v software.

Intracellular potassium assay

To measure intracellular potassium, 1×10^6 BMDMs were seeded overnight in 6-well plates and the medium was replaced with Opti-MEM supplemented with 1% FBS and ultrapure LPS (50 ng/mL) for 3 h. The cells were treated with DMSO or different concentrations of inhibit for 30 min and then stimulated with 5 μM nigericin for 30 min. The medium was removed and the cells were lysed with 3% ultrapure HNO3. Intracellular K^+ measurement was performed by inductively coupled plasma optical emission spectrometry (ICP-OES) with a PerkinElmer Optima 2000 DV spectrometer using yttrium as the internal standard.

Intracellular chloride assay

To measure intracellular chloride, 5×10^5 BMDMs were seeded overnight in 12-well plates. and the medium was replaced with Opti-MEM supplemented with 1% FBS and ultrapure LPS (50 ng/mL) for 3 h. The cells were treated with DMSO or different concentrations of inhibit for 30 min and then stimulated with 5 μM nigericin for 30 min. The medium was removed and the cells were lysed with ddH_2O. Then, cell lysate was collected and centrifuged at 10,000 × g. Transferred the supernatants to a 1.5 mL EP tube and mixed with 50 μL MQAE (10 μM). The absorbance was examined by BioTek Multi-Mode Microplate Readers (Synergy2).

Immunoprecipitation

For endogenous immunoprecipitation assay, BMDMs were seeded in 6-well plates and stimulated with nigericin after DMSO or inhibitor treatment, and then the BMDMs were lysed by NP-40 lysis buffer (pH 7.4, 150 mM NaCl, 50 mM Tris, 2 mM EDTA, 0.5% Nonidet P-40) with complete protease inhibitor. The cell lysates were incubated with anti-ASC or anti-NEK7 antibodies and Protein G resin overnight at 4°C and then were assessed by western blotting.

For exogenous immunoprecipitation assay, HEK-293T cells were seeded in 6-well plates and transfected with plasmids via Lipofectamine 2000 for 24 h. The cells were collected and lysed by cold NP-40 lysis buffer with complete protease inhibitor. Extracts were immunoprecipitated with Flag-M2 monoclonal antibody–agarose beads and then were assessed by western blotting.

Drug affinity responsive target stability (DARTS) assay

BMDMs pre-stimulated with 50 ng/mL LPS for 3 h and HEK-293T cells transfected with WT or mutant NEK7 plasmids for 24 h. The cells were lysed with NP-40 lysis buffer (pH 7.4, 150 mM NaCl, 50 mM Tris, 2 mM EDTA, 0.5% Nonidet (P-40) containing complete protease inhibitor. Lysates were centrifuged at 10,000 × g for 10 min at 4°C and the concentration of protein was measured by the Pierce BCA Protein Assay Kit (Beyotime). The lysates were incubated overnight with ENB in rotation at 4°C, followed by the addition of protease pronase (25ng enzyme per μg protein, Sigma) for 30 min at room temperature. The reaction was stopped after 3×SDS loading buffer was added and then the samples were analyzed by immunoblotting.

Cellular thermal shift assay (CETSA)

5×10^5 BMDMs were seeded overnight in 6 cm dishes and then treated with DMSO or ENB for 2 h. The cells were washed twice and resuspended with 500 μL PBS. The lysates were divided into 8 servings and loaded into the PCR tubes (50μL/tube), and then the samples were treated with temperature gradients (40, 43, 46, 49, 52, 55, 58, and 61°C) for 5 min followed by cooling on dry ice. The lysates were transfered to new tube and centrifuged at 20,000 × g for 20 min at 4°C. The supernatants were added 3×SDS loading buffer and analyzed by immunoblotting.

In vitro kinase activity assay

The kinase activity assay of NEK7 was performed as previously described.[66] Briefly, recombinant NEK7 and its substrate β-casein (Sigma-Aldrich, C6905) were co-incubated in the presence or absence of entrectinib. The kinase activity was analyzed according to the manufacturer's instructions of the Kinase Activity Kit (R&D Systems, EA004).

LPS-induced systemic inflammation

Ten-week-old male C57BL/6 mice were intraperitoneally injected with vehicle or ENB (10 mg/kg) for 1 h before intraperitoneally injected with 20 mg/kg LPS (Sigma Aldrich) to induce systemic inflammation. Serum samples were collected 6 h later and centrifuged at 3000 r/min for 15 min. ELISA was used to detect the levels of IL-1β and TNF-α according to the manufacturer's protocol. The levels of aspartate aminotransferase (AST) and alanine aminotransferase (ALT) in serum were measured using ALT and AST assay kits (Jiancheng, Nanjing China). Liver samples were histologically assessed by H&E staining.

MSU-induced peritonitis

The mouse model of MSU-induced peritonitis was performed as previously described.[67] Briefly, ten-week-old C57BL/6 mice were intraperitoneally injected with vehicle or ENB (10 mg/kg) for 1 h before intraperitoneally with MSU (1 mg/mouse, Sigma Aldrich). After

6 h, mice were sacrificed and peritoneal cavities underwent lavage with 5 mL cold PBS. Peritoneal lavage fluid was assessed by flow cytometry (BD) with the neutrophil markers Ly6G and CD11b for analysis of the recruitment of neutrophils and determined IL-1β production by ELISA.

High-fat diet (HFD) and ENB treatment

Six-week-old C57BL/6 mice with similar body weights were randomly divided into different experimental groups. For ENB prevention research, C57BL/6J mice were fed with 60 kcal% HFD from the start of the experiment until week 16, along with intraperitoneal injection of vehicle or ENB (1 mg/kg) every two days. For ENB therapy research, C57BL/6J mice were first fed with 60 kcal% HFD for 12 weeks and then intraperitoneal injection of vehicle or ENB (1 mg/kg) once a day for 4 weeks.

Glucose tolerance or insulin tolerance test

For glucose tolerance test (GTT), mice were fasted for 14 h and then intraperitoneal (i.p.) injection of glucose at 1.5 g/kg for C57BL/6J mice. Glucose levels at different time points in blood collected from the tail vein were measured by using a One Touch Ultra Blood Glucose Test System Kit (Lifespan Company, USA).

For insulin tolerance test (ITT), mice were fasted for 4 h and then intraperitoneal (i.p.) injection of human recombinant insulin (Novo Nordisk) at dose of 1 IU/kg for C57BL/6J mice. Blood glucose levels were measured from the tail veil at 15, 30-, 60-, 90- and 120-min following insulin injection.

Histological analysis

Fresh mouse liver tissues were fixed in 4.0% formalin buffer for 24 h to stabilize the tissue and sectioned after embedding in paraffin. The sections with a thickness of 4 μm were stained with hematoxylin and eosin (H&E) or Oil red O using standard procedures. The slides were examined by Nikon ECLIPSE Ci biological microscope and images were captured with a NikonDS-U3 color digital camera.

QUANTIFICATION AND STATISTICAL ANALYSIS

All statistical analyses were done using GraphPad Prism V9 software and data are presented as the mean ± SEM. Normality test was conducted using Shapiro–Wilk test in the SPSS software and all data points followed a normal distribution. Statistical analysis was carried out with the unpaired Student's *t* test for two groups, one-way ANOVA for multiple groups or two-way ANOVAs for groups containing two elements. No data points were excluded. Sample sizes were selected on the basis of preliminary results to ensure adequate power. Data were considered significant when the p value <0.05.